THESIS

QUANTIFYING LAWN IRRIGATION CONTRIBUTIONS TO SEMI-ARID, URBAN STREAM BASEFLOW WITH WATER-STABLE ISOTOPES

Submitted by

Noelle K. Fillo

Department of Civil and Environmental Engineering

In partial fulfillment of the requirements

For the Degree of Master of Science

Colorado State University

Fort Collins, Colorado

Spring 2020

Master's Committee:

Advisor: Aditi S. Bhaskar

Ryan T. Bailey
Stephanie K. Kampf

ABSTRACT

QUANTIFYING LAWN IRRIGATION CONTRIBUTIONS TO SEMI-ARID, URBAN STREAM BASEFLOW WITH WATER-STABLE ISOTOPES

In semi-arid cities, urbanization can lead to elevated baseflow during summer months. One potential source for the additional water is lawn irrigation. We sought to quantify the presence of lawn irrigation in Denver's summertime baseflow using water-stable isotope ($\delta^{18}O$ and $\delta^{2}H$) analysis of surface water, tap water, and precipitation. If lawn irrigation contributed significantly to baseflow, we predicted the isotopic composition of Denver's urban streams would more closely resemble the local tap water than precipitation or streamflow from nearby grassland watersheds. We expected the tap water to be distinctive due to local water providers importing much of their source water from high elevations. Thirteen urban streams and two grassland streams were selected for sampling. The thirteen urban watersheds ranged from 3.9 km^2 - 63.3 km^2 in drainage area and 22% - 44% in imperviousness. The two grassland watersheds had drainage areas of 3.7 km^2 and 7.5 km^2 as well as 1% and 5% imperviousness. None of the streams had high-elevation headwaters or wastewater effluent, and the grassland streams did not receive irrigation. Tap water was sampled from five local water provider service areas. Wide spatial and temporal variation in isotopic composition was observed within the stream, tap and precipitation samples. Comparison of samples between nearby watersheds revealed that proximity did not imply similar isotopic values. Streamflow analysis focusing on summer 2019 revealed that the grassland watersheds flowed for 60% of the summer while urban watersheds flowed for 90% - 100% of the summer. A two end-member isotope mixing model using tap and precipitation end-members estimated that tap water contributed 61% - 97% of urban streamflow on specific days in late summer. After taking estimated contributions from infrastructure leakage into account, we conservatively determined the lawn irrigation return flows made up 4% - 75% of the modeled baseflow. Quantifying the contribution of lawn irrigation to urban baseflow

will provide a basis for understanding how changes to lawn irrigation efficiency would affect water yield in the Denver metropolitan area.

ACKNOWLEDGEMENTS

Completion of this work would not have been possible without my graduate adviser, Dr. Aditi Bhaskar. She went above and beyond to ensure I had the resources needed to succeed both in and beyond the university, and her kind, brilliant personality made her a joy to work with. I owe much of my professional and personal development made while conducting my research to her, and I am grateful for her support and guidance on this journey.

My thanks also go out to Dr. Ryan Bailey and Dr. Stephanie Kampf for being members of my master's committee. I appreciate them taking the time to read about and providing valuable feedback on my research. Their input was crucial in creating a compelling thesis presentation.

I would also like to thank the network of people who assisted me with data collection and other necessary tasks. Ryan Baird, Aditi Bhaskar, Ben Choat, Anne Jefferson, Katie Knight, Shannon Petts, Noah Sandoval, Connor Williams, and Wyatt Young were essential for project success. I wish them all the best in their future endeavors and cannot wait to see how they change the world.

This work was supported by the USDA National Institute of Food and Agriculture, Hatch project 1015939.

TABLE OF CONTENTS

Chapter 1: Introduction

Water scarcity has forced semi-arid and arid cities to be conscious of how local water resources are managed and has historically acted as a barrier to urban growth (ARUP, 2018). One strategy that older urban regions have used to overcome the limitations of local water reserves is to import their drinking water from elsewhere. Modern cities continue to fight against water scarcity with innovative solutions such as improving the efficiency of water technologies, treatment/reuse of wastewater, rainwater harvest, and climate-conscious water planning (Gleick, 2010). These strategies have helped weaken the growth barrier allowing more land to be developed. However, the conversion of land from natural/agricultural use to urban use has the potential to significantly alter hydrologic conditions in a variety of ways. Streamflow and ecosystem responses to urbanization have been shown to vary across the United States, which establishes the need for water management plans tailored to individual urban complexes (Hopkins *et al.*, 2015; Coles *et al*., 2012).

Hopkins *et al.* (2015) noted that explaining the relationship between urbanization and baseflow (also called low flow or dry-weather flow) was exceptionally difficult. Further exploration of this relationship revealed that post-development baseflow has the potential to rise, fall, or remain consistent when compared to pre-development observations (Bhaskar *et al.,* 2016). Potential urban causes of rising baseflow include wastewater effluent outfalls, channel deepening and riparian vegetation removal (Hibbs *et al.*, 2012), irrigation ditch/canal inputs, leaking water infrastructure (Lerner, 1990; Garcia-Fresca & Sharp, 2005), and lawn irrigation return flows (Manago & Hogue, 2017).

Lawn irrigation return flows (LIRFs) are defined as water originally intended for plant growth that is instead transported to streams via alternative flow paths of (1) surface runoff into a storm sewer system, which then drains to a local stream; (2) infiltration of irrigation to saturated zone and subsequent discharge from the subsurface to a stream; or (3) surface runoff from lawn irrigation entering directly into a stream (Figure 1). Considering LIRFs and other forms of outdoor water use in urban water policy, conservation, planning, and management can help cities in dry climates become more resilient to the

unpredictability associated with climate change (Gober *et al.*, 2015). There are only a few studies that quantify the effect of LIRFs to semi-arid streamflow, but efforts to quantify LIRFs have found them to be important. Manago and Hogue (2017) found that streamflow in an urban watershed in Los Angeles was 7 times larger compared to streamflow in a nearby undeveloped watershed prior to the implementation of drought restrictions. These drought restrictions reduced the amount of water that could be used for lawn irrigation. Urban streamflow dropped by 70% during the restriction period, while the non-urban watershed experienced no statistically-significant changes in streamflow.

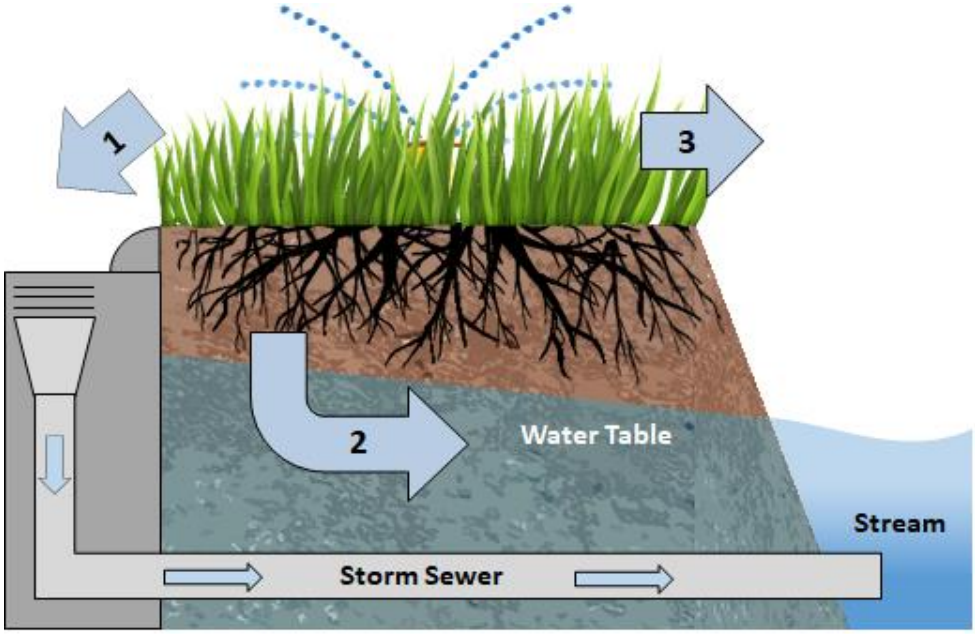

Figure 1. A diagram showing three potential pathways for lawn irrigation return flows to enter rivers. 1: surface runoff into storm sewer system, which then drains to local stream; 2: infiltration of irrigation to saturated zone and subsequent discharge from subsurface to stream; 3: surface runoff directly into stream.

The semi-arid, growing, urban area of Denver, Colorado, USA receives an average annual precipitation of 396 mm and may be an area where LIRFs are important contributors to stream baseflow (National Oceanographic and Atmospheric Administration, 2020). Denver and its surrounding cities have experienced significant urbanization over the past 58 years in response to a 226% increase in population between 1960 and 2018, and the impact this has had on local baseflow has yet to be determined (United States Census Bureau 1996; United States Census Bureau 2019). In Denver, 62% of residential water is

used outdoors and 74% of surveyed homes had "in-ground irrigation/sprinkling systems," mostly with automatic timers (DeOreo *et al.*, 2016).

Assessments of the contributions from different sources to streamflow can be performed by various methods, including the use of isotope tracers. Water-stable isotope analysis quantifies the relative proportions of naturally-occurring hydrogen ($^{2}H/^{1}H$) and oxygen ($^{18}O/^{16}O$) isotopes to inform water provenance and processes. It is possible to determine water sources and processes experienced by the water since isotopologues of water have different atomic weights and sizes, which causes isotopes to partition, or *fractionate*, during phase changes (Kendall & McDonnell, 1998). Because of this, water-stable isotopes have been applied to understand evaporation trends in large river systems (Simpson & Herczeg, 1991) and the effects of urbanization in semi-arid regions (Ehleringer *et al*., 2016). When sources have distinct isotopic signatures, use of isotope tracers allow for these source contributions to streamflow to be measured directly on an integrated, watershed-wide basis. Other methods, such as use of water balance approaches, do not allow for direct measurement of contributions, instead relying on estimates of water balance components with large uncertainties and are often assumed to be spatially- or temporally- constant. Water isotopes can also help pinpoint sources with much more specificity than a typical water balance can feasibly identify, such as flow that passed through a particular stormwater control measure (SCM) before entering a stream (Jefferson *et al.*, 2015).

Our goal was to answer the following questions: (1) how much of Denver's summertime baseflow comes from tap water sources and (2) how much of the tap water contribution can be attributed to lawn irrigation compared to other sources of tap water. We planned to answer these questions using water-stable isotopes as environmental tracers of provenance and processes undergone. Surface water from urban and grassland watersheds was compared to tap water and precipitation to determine the relative contributions to Denver baseflow. If lawn irrigation contributes significantly to baseflow, we predicted the isotopic composition of Denver's urban streams would more closely resemble the local tap water than streamflow from nearby grassland watersheds. We expected the tap water to be distinctive

since local water providers do not source their tap water locally. Instead, much of the Denver metropolitan area's tap water is imported from high-elevation collection areas.

Chapter 2: Methods

2.1 Study Area Characterization

Thirteen urban watersheds and two grassland watersheds in the Denver Metropolitan area were included in the study (Figure 2, Table 1). The watersheds were delineated using the National Hydrography Dataset (with a stream segment modification in the SWOM grassland watershed) and a 10 m digital elevation model (United States Department of Agriculture, 2018) in ArcGIS Pro. Watershed outlets, representing stream sampling locations, for the urban streams coincided with United States Geological Survey (USGS) stream gage locations. The USGS stream gages were maintained from April 1 to September 30 each year. Our analysis required mean daily streamflow data supplied by these gages, so we were only able to use samples taken during that timeframe. The grassland watersheds were located in the Rocky Flats National Wildlife Refuge. The outlets for the grassland watersheds were chosen based on proximity to walking trails and a United States Department of Energy (DOE) stream gage. Neither canals nor stormwater networks were included in the delineation. All of the watersheds lacked high-elevation headwaters, and the Environmental Resource Assessment and Management System (eRAMS) GIS tool confirmed that there were no wastewater treatment plants discharging effluent into our watersheds (Catena Analytics, 2019). The mean elevations of our study watersheds ranged from 1628 m - 1891 m above sea level. The grassland streams did not receive any irrigation.

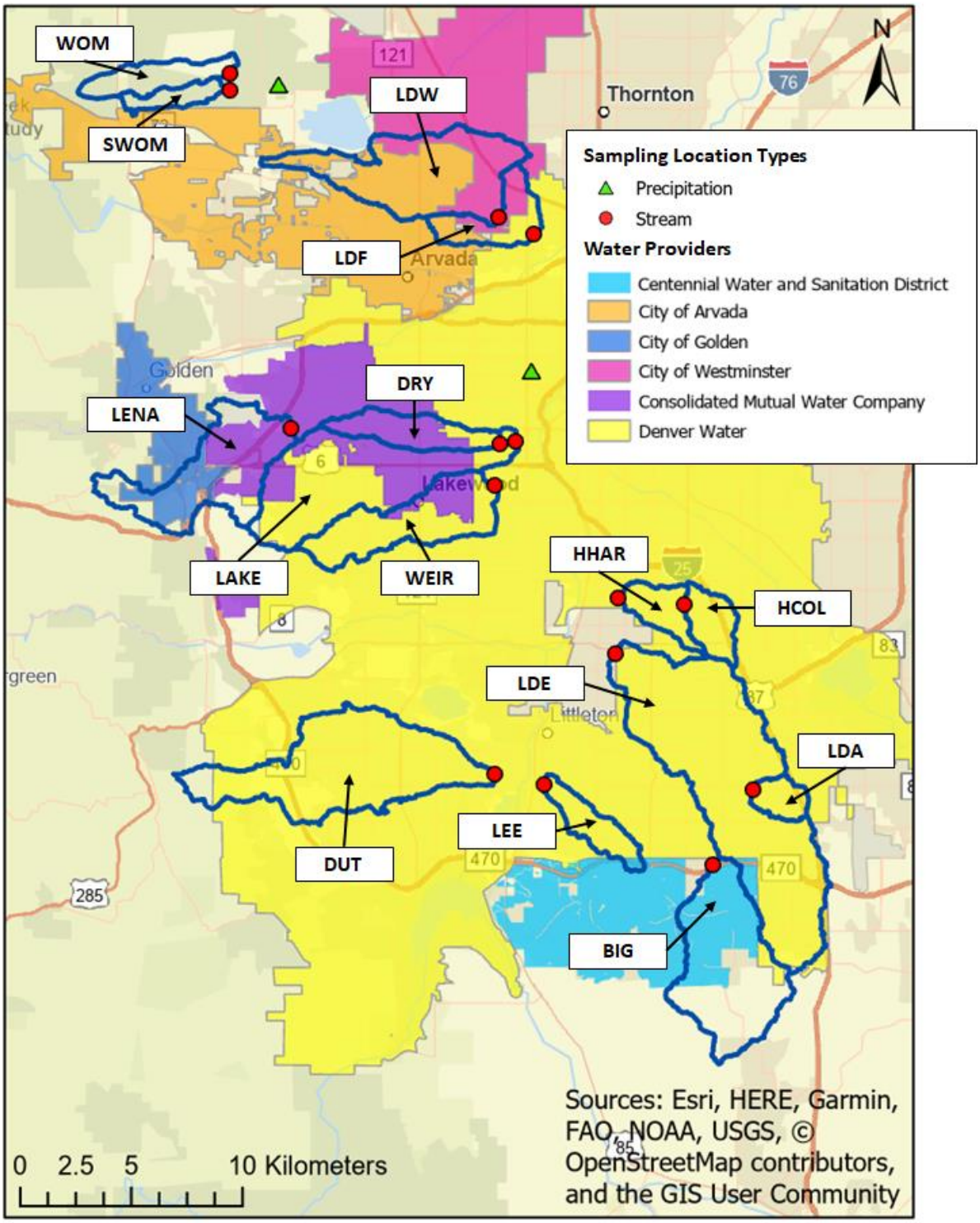

Figure 2. Map of the study grassland and urban watersheds (Table 1), stream sampling locations, precipitation sampling locations, and water provider boundaries in the Denver Metropolitan Area.

Table 1. Watershed characteristics.

Abbreviation Used Here	Name	Type	Gage Authority	Gage ID	Drainage Area (km^2)	Impervious - ness (%)
BIG	Big Dry Creek - Highlands Ranch	Urban	USGS	06710150	29.4	22
DRY	Dry Gulch - Denver	Urban	USGS	06711770	9.1	42
DUT	Dutch Creek - Littleton	Urban	USGS	06709910	38.1	26
HCOL	Harvard Gulch - Colorado Blvd.	Urban	USGS	06711570	5.9	36
HHAR	Harvard Gulch - Harvard Park	Urban	USGS	06711575	11.6	32
LAKE	Lakewood Gulch - Denver	Urban	USGS	06711780	40.7	34
LEE	Lee Gulch - Littleton	Urban	USGS	06709740	6.5	29
LENA	Lena Gulch - Lakewood	Urban	USGS	06719560	23.8	24
LDA	Little Dry Creek - Arapahoe Rd.	Urban	USGS	06711515	3.9	44
LDE	Little Dry Creek - Englewood	Urban	USGS	06711555	63.3	29
LDF	Little Dry Creek - Federal Blvd.	Urban	USGS	06719845	36.7	35
LDW	Little Dry Creek - Westminster	Urban	USGS	06719840	28.1	33
SWOM	South Woman Creek / Smart Ditch	Grassland	N/A	N/A	3.7	1
WEIR	Weir Gulch - Denver	Urban	USGS	06711618	18.6	32
WOM	Woman Creek	Grassland	DOE	WOMPOC	7.5	5

The Denver metropolitan area was serviced by multiple tap water providers: Centennial Water and Sanitation District, City of Arvada, City of Golden, City of Westminster, Consolidated Mutual Water Company, and Denver Water (Figure 2). To identify the service area boundaries, GIS shapefiles for each water provider's service area boundaries were downloaded from public GIS databases or requested from the water providers. Several of the shapefiles had to be edited to account for recent service area changes, and the shapefile for Consolidated Mutual Water Company had to be hand-digitized based on an image of the service area located on the company website (Consolidated Mutual Water Company, 2019). The shapefile for Highlands Ranch Metro District was used to represent the Centennial Water and Sanitation District service area since only the Highlands Ranch Metro District portion of the Centennial Water and Sanitation District service area was considered in the annual water loss reports (see Methods section 2.6 for more details).

In addition to water provider service area boundaries (Figure 2), we were also interested in the collection areas for these water providers. These water providers, besides Centennial Water and Sanitation District, imported their water exclusively from high-elevation watersheds (Figure 3). Additional collection areas for the other water providers were calculated using the StreamStats web application (United States Geological Survey, 2020). Denver Water's collection areas had mean elevations ranging from 2622 m – 3556 m above sea level and consisted of the Williams Fork, Roberts Tunnel, South Platte, Moffat, and Wolford Mountain watersheds (Leonard Rice Engineers, Inc., 2015). The City of Golden and the City of Westminster sourced their tap water from the Clear Creek watershed, which had a mean elevation of 3036 m above sea level (City of Golden, 2020; City of Westminster, 2017; United States Geological Survey, 2020). The City of Arvada sourced its water from both the Clear Creek watershed as well as Denver Water's Moffat collection region, which had a mean elevation of 3556 m above sea level (City of Arvada, 2005; Leonard Rice Engineers, Inc., 2015). Consolidated Mutual Water Company received water from the Clear Creek, Moffat, and Coal Creek watersheds (Consolidated Mutual Water Company, 2020). The Coal Creek watershed had a mean elevation of 2516 m above sea level (United States Geological Survey, 2020). Centennial Water and Sanitation District was the only water

provider within our study area that used a combination of surface water from the South Platte River and deep groundwater (Centennial Water and Sanitation District, 2012). The mean elevation of the South Platte watershed was 2831 m above sea level (Leonard Rice Engineers, Inc., 2015).

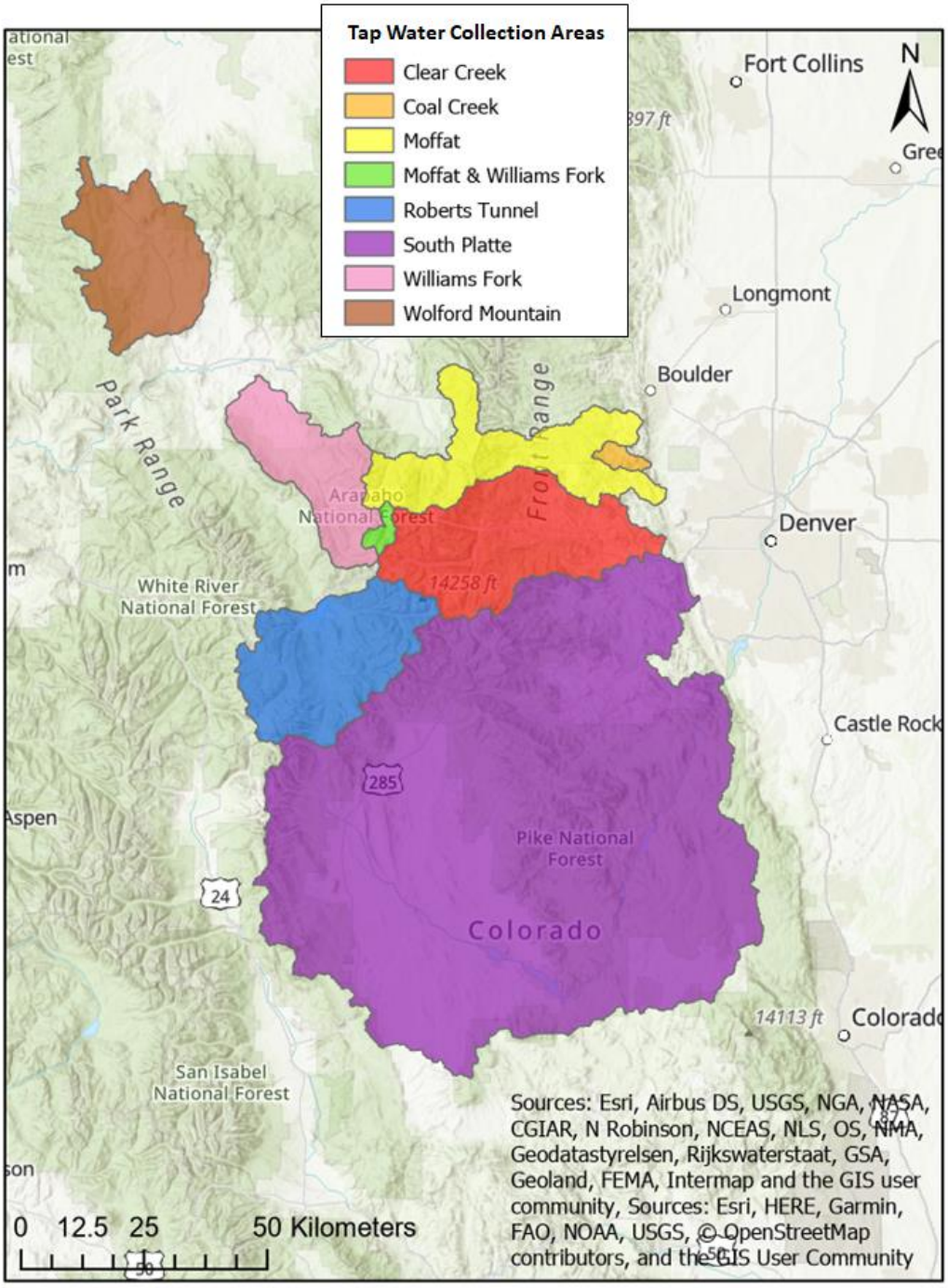

Figure 3. Map of high-elevation tap water collection areas for water providers in the Denver Metropolitan area.

In an effort to capture spatial variability in the study area precipitation, two precipitation locations were chosen (Figure 2). Global Network of Isotopes in Precipitation (GNIP) recommendations for precipitation isotope sampling, such as locating precipitation samplers away from large trees or buildings, were followed when establishing sampling sites (Global Network of Isotopes in Precipitation & International Atomic Energy Agency, 2014). The first precipitation sampler was deployed in March 2019, and the second precipitation sampler was deployed in May 2019.

A supervised land cover model was generated using a random forest classification algorithm in Google Earth Engine to calculate the percent imperviousness for each watershed. A 1 m resolution 2015 image provided by the National Agriculture Imagery Program (NAIP) was used in the classification, and roads, parking lots, buildings, and swimming pools were all considered when determining percent imperviousness. We compared the percent imperviousness calculated in the model with the percent imperviousness calculated using the USGS StreamStats tool to evaluate the performance of the model (Table A5). We assumed that shadows in the imagery had negligible effects on the classification.

2.2 Sample Collection and Storage

One hundred ninety-two streamflow, tap water, and composite precipitation samples were taken throughout the Denver metropolitan area in September 2018 and between March 23, 2019 and October 1, 2019 (Tables A1 – A7). Sampling was often conducted in public spaces, so appropriate safety and ethical guidelines were followed when in public urban spaces per Dyson *et al.* (2019). We sampled streams under well-mixed flow conditions to ensure individual samples were representative of their respective water columns. We took stream samples approximately biweekly as long as baseflow was present. To ensure only baseflow was captured, we conducted sampling three or more days after recent precipitation events and examined current flow conditions using USGS hydrographs. Stream samples were collected in 60 mL clear plastic bottles. These bottles were chosen since the clear cap and bottle helped verify if any air had been caught in the capture process.

Tap sampling sites were often located in restaurant or gas station bathrooms. Initially, (between September 2018 and July 2019), we collected one tap sample per week and the sampling location was

simply based on proximity to stream sampling locations. In August 2019, we noticed spatial and temporal variability among tap samples (presented in the Results and Discussion sections), and modified our sampling strategy to choose one tap sampling location within each watershed we were planning to sample on a given day. We collected cold water when the option was available; we occasionally sampled from automatic faucets. Tap samples were collected in the same type of bottles as the stream samples. Twenty-five additional tap data points in our study area were downloaded from the Waterisotopes.org database and included in the study (University of Utah, 2019).

Composite (volume-weighted) precipitation samples were collected on a monthly basis. Precipitation was collected in a 3 L plastic bottle using a commercial precipitation isotope sampler (Rain Sampler RS1, Palmex Ltd.). The sampler was designed to prevent evaporation and isotopic fractionation during storage (Palmex Ltd., 2019). The snow tube attachment for the sampler was used for the entire season. All samples were immediately placed in an iced cooler post-collection for transport back to Colorado State University. Samples were kept in a refrigerator that maintained a constant temperature of 4°C until it was time to send samples out for analysis.

2.3 Sample Preparation and Analysis

The University of Utah's Stable Isotope Ratio Facility for Environmental Research (SIRFER) laboratory was used for all of our isotopic analyses. Prior to overnight chilled shipment to the SIRFER laboratory, samples were filtered through 0.2 μm filters into 1.8 mL crimp-sealed glass vials per laboratory specifications (SIRFER, 2020). We assumed that no isotopic fractionation occurred any time post-sample capture. Samples were analyzed at SIRFER within two months of sample reception using cavity ring-down spectroscopy (L2130-i, Picarro Inc.) as well as pyrolysis-driven isotope ratio mass spectroscopy (TC/EA, Thermo Finnigan; Delta V IRMS, Thermo Finnigan). Necessary carbon dioxide and hydrogen gas equilibration was also performed during analysis (GasBench II, Thermo Finnigan; MAT 253 IRMS, Thermo Finnigan).

The output of these techniques is in the form of an isotope ratio δ which is derived from the molar ratio R. R values are calculated by juxtaposing the abundances of a less-common stable isotope to the most common stable isotope of a given element:

$$R_{sample} = \frac{R_{Less-Common}}{R_{Common}} \quad (1)$$

For our analysis, these ratios were calculated by comparing the abundances of ^{2}H to ^{1}H and ^{18}O to ^{16}O. The R ratio is then compared to the Vienna Standard Mean Ocean Water (VSMOW) R value to find the isotope ratio which is given in units of permille (parts per thousand):

$$\delta[‰] = (\frac{R_{sample}}{R_{VSMOW}} - 1) \times 1000 \quad (2)$$

SIRFER analytical precisions associated with each isotope ratio are 0.2‰ for $\delta^{18}O$ and 2‰ for $\delta^{2}H$ (Cook *et al*. 2018). The measured reference uncertainties associated with QA/QC for all isotope analysis batches had ranges of 0.0 - 0.1‰ for $\delta^{18}O$ and 0.0 - 0.3‰ for $\delta^{2}H$.

2.4 General Data Analysis

After receiving results from the SIRFER laboratory, we compared our precipitation isotope measurements against the global meteoric water line (GMWL), local meteoric water line (LMWL), mean annual precipitation isotope signature, and mean monthly isotope signatures. The isotope ratios of our measured samples and the downloaded samples were also compared to the GMWL, over time, and against watershed characteristics of drainage area, percent imperviousness, elevation, and slope using R Studio. Only 182 of the 192 data points we collected were used in our analysis. The five samples taken on September 10, 2018 were taken in duplicate, and we used the average values for those measurements in our investigation (Table A8). Five of our samples also broke or went missing during transit (Tables A9 and A10).

Since we were particularly interested in lawn irrigation, we wanted to link the isotope values and water providers. We calculated the percentage of service area(s) of each water provider contained in each watershed using the delineated watershed boundaries and the water provider boundaries in ArcGIS Pro (Tables A2 and A3). We then associated each tap sample with its water provider. Non-exceedance

probability graphs of area-normalized mean daily streamflow were created to allow for direct flow comparisons between watersheds of different sizes (United States Geological Survey, 2019; Navarro Research and Engineering, Inc., 2019).

2.5 Two End-member Mixing Model

We used a two end-member mixing model to calculate a range of precipitation and tap water proportions needed to yield the measured stream isotope value on a given day. Stream samples were selected for modeling if (1) six or more associated tap samples were taken within the two-week span prior to the stream sample collection date, (2) the associated tap samples were taken over multiple days, and (3) the stream isotope value was constrained between the average precipitation and tap isotope values over the two-week period (Figure 4). This assumed that stream samples were receiving input from tap water and precipitation from the previous two weeks. We considered tap samples from a specific water provider to be associated with a given watershed if the provider's service area covered more than one-third of the watershed area. These tap values were then grouped, and the mean, the mean plus one standard deviation, and the mean minus one standard deviation were used to calculate proportions in the end member mixing model. This was done to account for variation in the tap water samples (see Results section 3.4 for more details). The earliest and latest precipitation values over a two-week span were used in our model, and linear interpolation was used to calculate the precipitation values for days that fell between measurements. We used the mean precipitation values in our calculations when we had more than one precipitation measurement for a given month (June 2019 – September 2019).

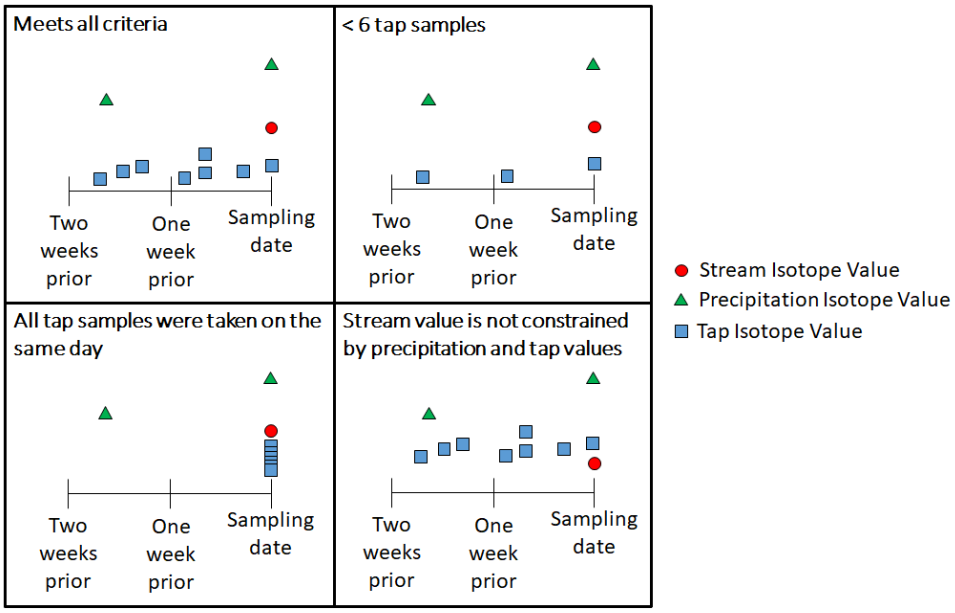

Figure 4. Diagram illustrating hypothetical stream samples that would meet or violate our criteria for inclusion in the mixing model.

The mixing model was built in Microsoft Excel and required solving the following two equations simultaneously:

$$\delta_{precipitation} \times Proportion_{precipitation} + \delta_{tap} \times Proportion_{tap} = \delta_{stream} \quad (3)$$

$$\left[Proportion_{precipitation} = \frac{Q_{precipitation}}{Q_{stream}}\right] + \left[Proportion_{tap} = \frac{Q_{tap\ water}}{Q_{stream}}\right] = 1 \quad (4)$$

$Proportion_{precipitation}$ and $Proportion_{tap}$ were the variables of interest (defined as flow derived from precipitation divided by streamflow and flow derived from tap water divided by streamflow, respectively) and $\delta_{precipitation}$, δ_{tap}, δ_{stream} represented the known precipitation, tap, and stream isotope ratios. Calculations were performed on the δ^2H and $\delta^{18}O$ tap samples (mean +/- one standard deviation) and precipitation samples (one or the mean of both samples) of the chosen days, and the resulting ranges were both considered when determining the overall estimated range of tap contributions to the urban streams.

2.6 Tap Contribution Characterization

We sought to estimate lawn irrigation contributions to streamflow, but the above mixing model gives us tap water contributions to streamflow. In addition to lawn irrigation, other possible sources of tap water to streamflow may be through leaking water distribution infrastructure or wastewater effluent. Wastewater effluent was not present in our study streams. To estimate the leakage from water distribution

infrastructure in each watershed and compare the magnitude to streamflow, we first obtained reports detailing annual infrastructure water losses for each water provider (Colorado Water Conservation Board, 2018). The 2019 water provider reports were unavailable, so we used 2018 infrastructure loss values for our calculations (Tables A11 and A12). These losses overestimate leakage as they also include unauthorized use. The annual losses (e.g., acre-ft/yr and thousand gal/yr) were divided by the total service area considered in the report to get area-normalized annual loss depths. These depths were then multiplied by the service area coverage proportion(s) for each watershed and added to get an overall annual loss depth for the watershed. This annual loss depth was then converted to a daily loss depth. Without other information, we assumed the infrastructure loss contributions would be uniform across the service area and throughout the year. The area considered for the water provider loss reports did not always coincide with the entire service area, so reporting areas were confirmed via direct contact with report writers (Beckwith, D., personal communication, January 16, 2020; Essert, W., personal communication, January 16, 2020; Stambaugh, personal communication, January 18, 2020; Riggle, personal communication, January 16, 2020; Weismiller, K, personal communication, February 12, 2020). Most of Consolidated Mutual Water Company's service area was included in Denver Water's loss report. Loss data from a small portion of Consolidated Mutual Water Company was not available, so we assumed the infrastructure losses for the reported area were equivalent to the losses from the unreported area. We then calculated the daily loss proportion that contributed to area-normalized mean daily streamflow (United States Geological Survey, 2019) and subtracted that proportion from the modeled tap contribution proportions to estimate the lawn irrigation proportion ranges.

Chapter 3: Results

3.1 Streamflow Comparison

Analysis of mean daily streamflow in the Denver Metropolitan area revealed that there were major differences in the non-exceedance probability curves of urban and grassland streamflow in the summer (April - September) of 2019 (Figure 5). The grassland stream was dry for almost 40% of the summer, while urban streams were dry for less than 10% of the summer. Eleven out of 13 urban streams had perennial flow. When there was flow present in the grassland stream, the area-normalized flow was overall lower than the urban streamflow across the non-exceedance probability curve. The urban streams further analyzed were chosen based on the criteria detailed in Methods section 2.4, and these streams were in the same streamflow range as the other urban streams (Figure 5).

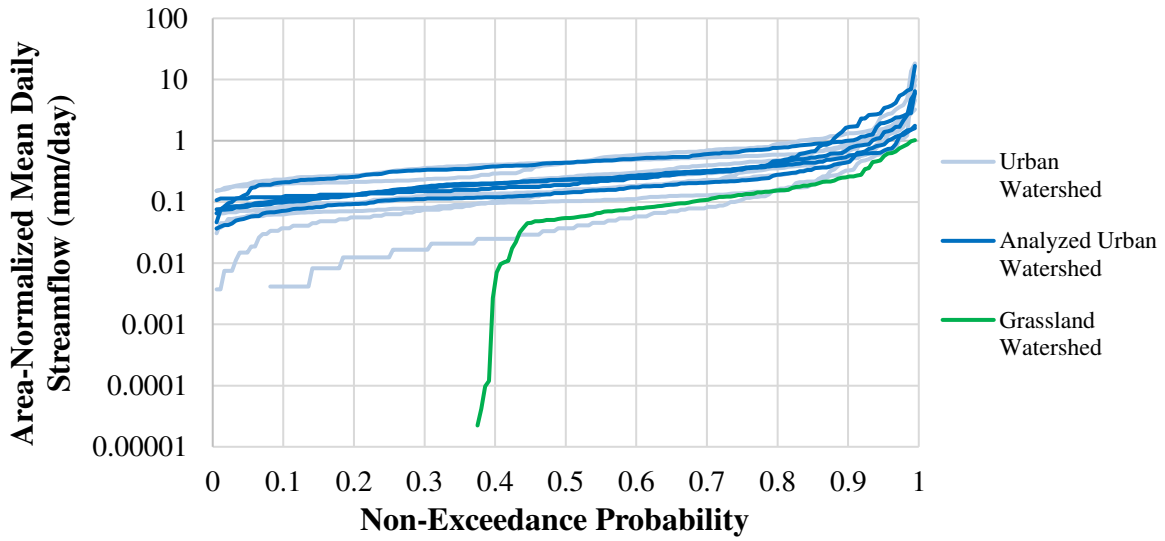

Figure 5. Non-exceedance probabilities for the 2019 area-normalized mean daily streamflow in the Denver metropolitan area. Zero flow and unreported flow days are not shown on the logarithmic y-axis. Time frame is April 1, 2019 - September 30, 2019.

3.2 Water-Stable Isotope Relationships

Comparing isotope measurements to the GMWL can provide insight into local hydrologic systems. The GMWL represents the average annual precipitation isotope relationship observed globally (Craig, 1961). Deviation of individual precipitation isotopes from the GMWL is not uncommon and can

indicate climate conditions experienced by the isotopes. For example, points plotting below the GMWL can indicate the sampled water underwent evaporative processes (Kendall & McDonnell, 1998). Our measured precipitation isotope values dropped below the GMWL in June 2019 and remained below the GMWL through September 2019 (Figure 6). Since the Denver metropolitan area has a semi-arid climate, this observation was not unexpected. However, comparison to a local meteoric water line created using water-stable isotope data from the northeastern plains of Colorado suggested that our precipitation measurements were at times below both the LMWL and GMWL (Harvey, 2005). Mean annual and mean monthly precipitation isotope values from a modeled precipitation isotope grid (Bowen, 2020; Bowen *et al*., 2005; International Atomic Energy Agency, 2015; Welker, 2000) also plotted below the GMWL and LMWL for the months of June through September, although they were generally lower than our measured precipitation values (Figure 6).

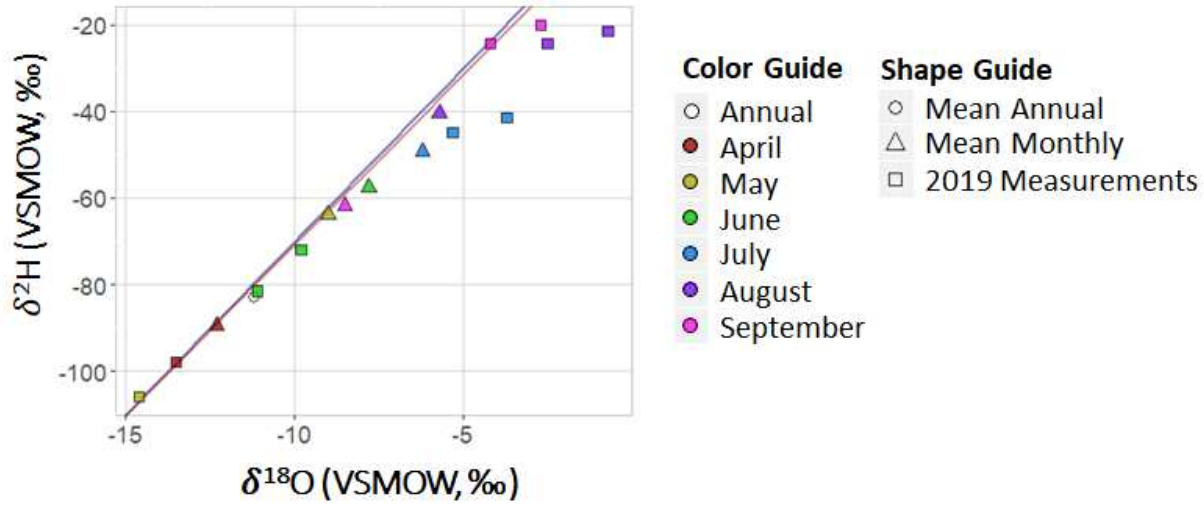

Figure 6. Plot comparing the ratios of δ^2H to δ^{18}O for mean annual, mean monthly (April – September), and our 2019 measurement for precipitation isotopes. The dark blue line represents the global meteoric water line (GMWL) and the brown line represents the local meteoric water line (LMWL) (Harvey, 2005). Mean annual and mean monthly values are from Bowen, 2020; Bowen *et al*., 2005; International Atomic Energy Agency, 2015; Welker, 2000.

Understanding the relationship between δ^2H and δ^{18}O can be useful in parsing isotopic signatures from specific water sources. The relationship between δ^2H and δ^{18}O was not consistent across all sample types (Figure 7). Tap and surface water samples consistently plotted below the GMWL while the precipitation samples plotted along the GMWL until July 2019. Like the precipitation samples, this

observation was expected since Denver's climate is semi-arid (Kendall & McDonnell, 1998). There was a consistent slope of the tap and surface water points throughout the summer and to each other, indicating the relationship between δ^2H and δ^{18}O was fairly stable among both sample types despite increases and decreases in the isotope values themselves (Figures 7b and 7c).

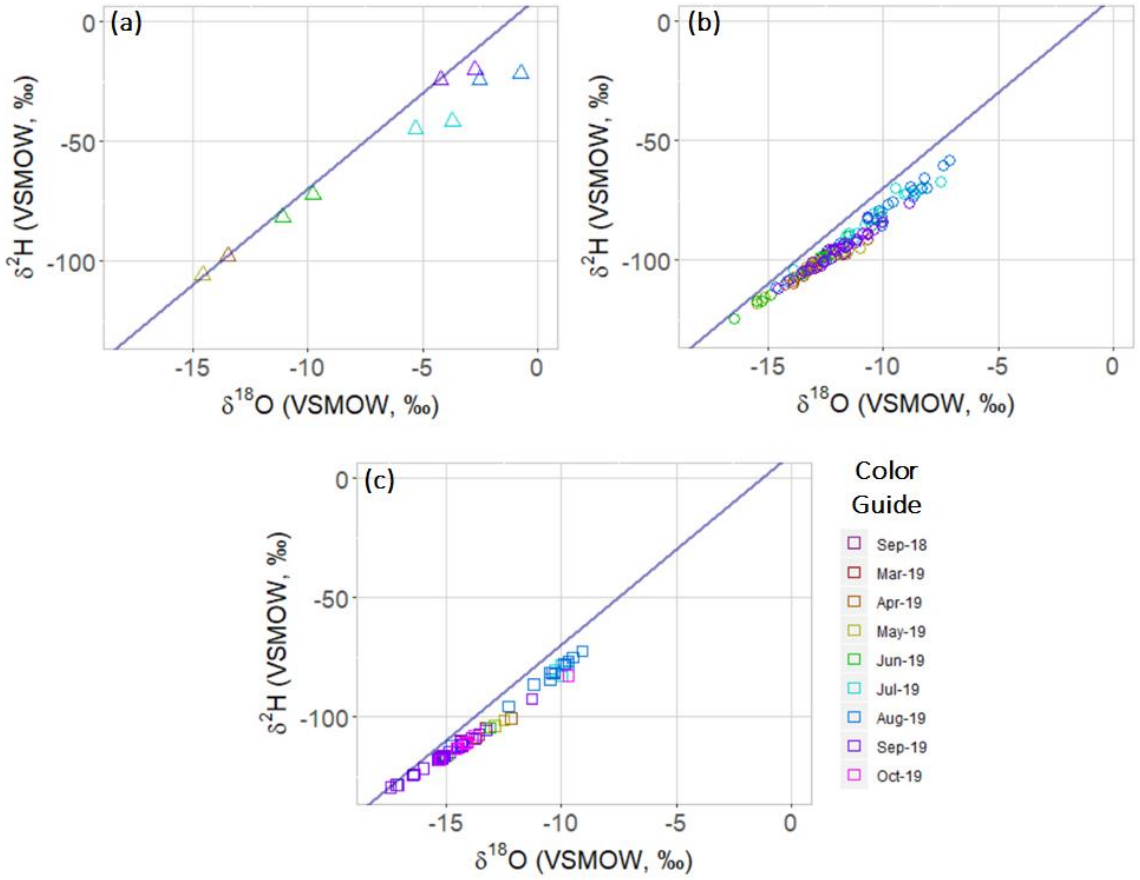

Figure 7. Plots comparing the ratios of δ^2H to δ^{18}O in (a) precipitation (b) surface water and (c) tap water. The dark blue line represents the global meteoric water line (GMWL).

The tap isotope values were similar to the stream isotope values for a given month (Figures 7b and 7c). The lowest isotope values were observed in the early (March - June) and late (August - September) summer months, and the highest isotope values were observed in July and parts of August. The precipitation values were similar to the tap and surface water values in the beginning of the summer, but the precipitation isotope values began rising in June and rose above the stream or tap samples. The

two precipitation samplers never yielded identical isotope values in the same month despite being 17.2 km away from each other.

3.3 Changes in Isotope Values over Time

Temporal and spatial variation was observed across all sample types and watersheds (Figure 8). The precipitation isotope values plotted along an increasing s-shaped curve while the tap and stream samples were generally flatter throughout the year with an increase in July - August. Urban stream, grassland stream, and tap isotope values plotted relatively close to the precipitation curves until early June. The exceptions to this pattern were watersheds DRY and LAKE (Figures 8b and 8f, respectively); they are both within the Consolidated Mutual Water Company service area and plotted below the precipitation curve. By July 2019, the grassland streams were no longer flowing and almost all stream and tap measurements displayed elevated isotope values. Stream and tap values also began to deviate from the precipitation curve in July. Stream and tap isotope values then dropped well below the precipitation curve in late August and remained low through the rest of the study period. Stream values plotted between the precipitation curve and the tap scatter or within the tap scatter at the end of the summer, with the sole exception of BIG on September 30, 2019 (Figure 8a). Despite our policy of waiting three days and checking for a trough on the USGS hydrographs, 20% of our stream samples may have contained stormflow (Figures A1 - A14). No linear relationships could be established between isotope values and watershed characteristics such as drainage area, percent imperviousness, elevation, watershed slope, or dominant water providers.

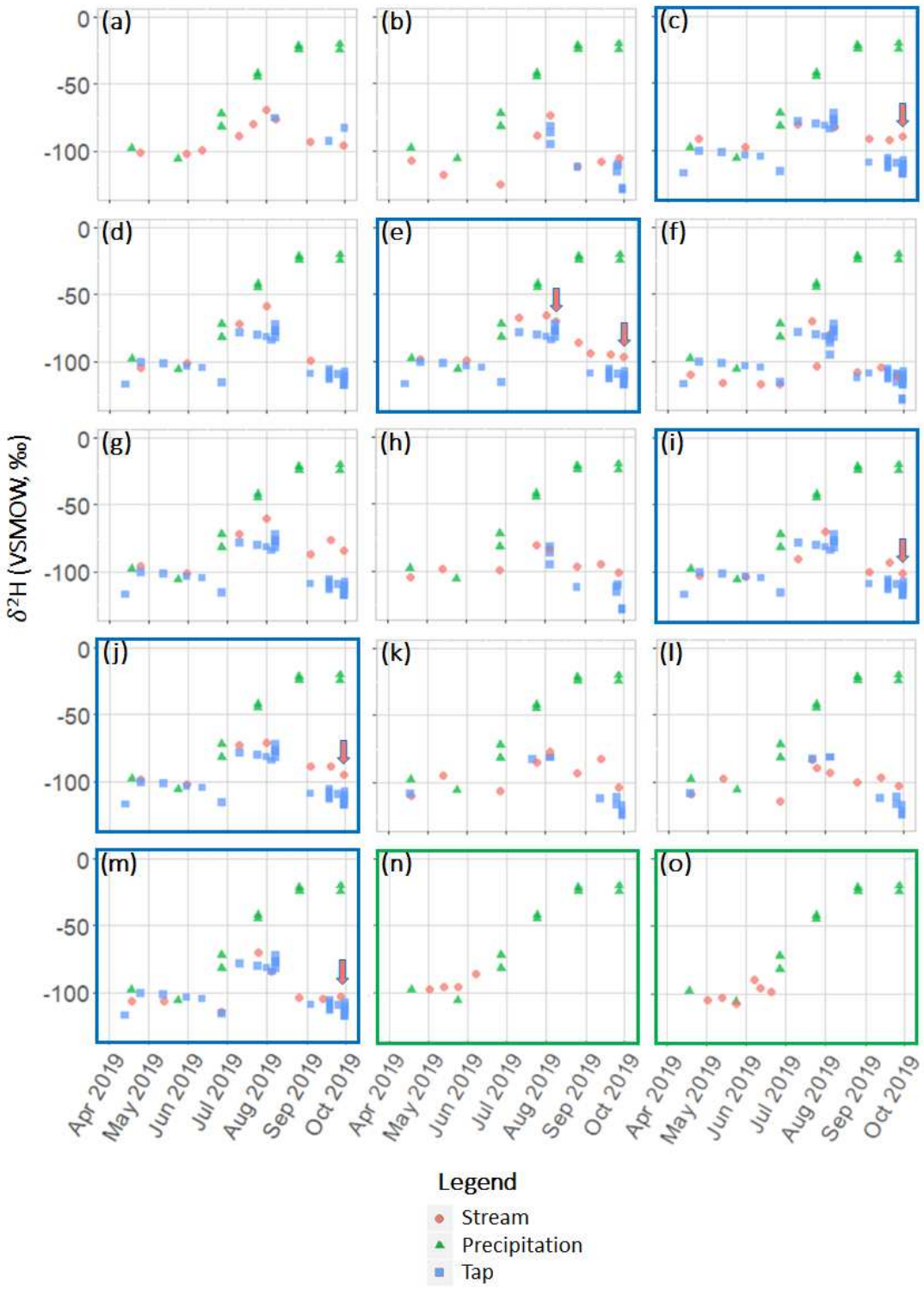

Figure 8. Changes in δ^2H over time for watersheds (a) BIG, (b) DRY, (c) DUT, (d) HCOL, (e) HHAR, (f) LAKE, (g) LEE, (h) LENA, (i) LDA, (j) LDE, (k) LDF, (l) LDW, (m) WEIR, (n) SWOM, and (o) WOM. Samples taken in September 2018 were not plotted due to temporal separation from the rest of the samples. Green boxes specify grassland watersheds and blue boxes specify urban watersheds chosen for analysis. Arrows indicate dates analyzed in Figure 11.

3.4 Tap Water Variation

The tap water in the Denver Metropolitan area displayed a surprising amount of variation. Samples from all water providers had elevated isotope values in July and early August, the same time as the stream samples (Figure 9). Tap samples taken on or around the same day within a single water provider did not yield identical isotope values. Consolidated Mutual Water Company isotope values typically plotted lower than most providers sampled on the same day, and Centennial Water and Sanitation District isotope values plotted higher than most providers sampled on the same day. More tap samples were taken between August 2019 and October 2019 because we altered our tap sampling strategy to better capture the variation within and between different water providers.

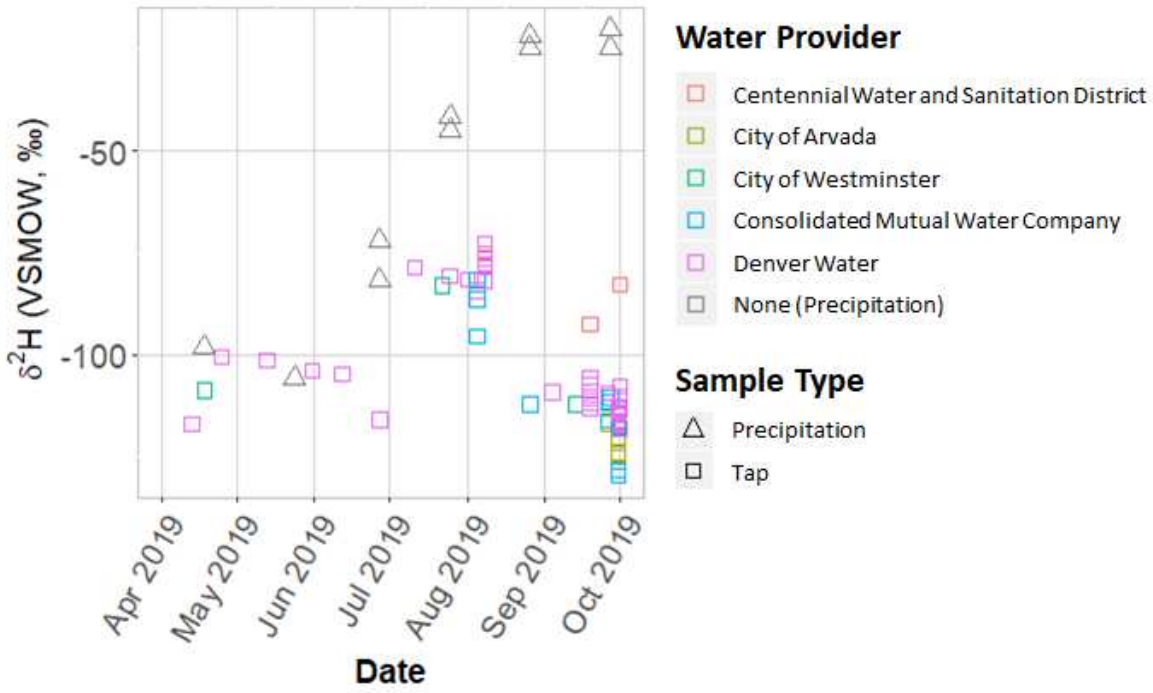

Figure 9. Changes in δ^2H over time for different tap water providers with precipitation samples shown for comparison.

The spreads of isotope values varied by water provider (Figure 10). The mean isotope values of Consolidated Mutual Water Company, Denver Water, and the City of Westminster were similar, but the City of Arvada's and Centennial Water and Sanitation District's means were lower and higher, respectively. Centennial Water and Sanitation District had the highest mean isotope values compared to

the other water providers. This is not surprising because it is the only water provider that uses groundwater sources versus surface water sources. The high values for Denver Water and the City of Arvada were associated with the elevated mid-summer phenomenon shown in Figure 9. Despite the observed variation between and within water providers, a substantial difference between late summer (September 2019) tap samples and local precipitation is apparent (Figure 9).

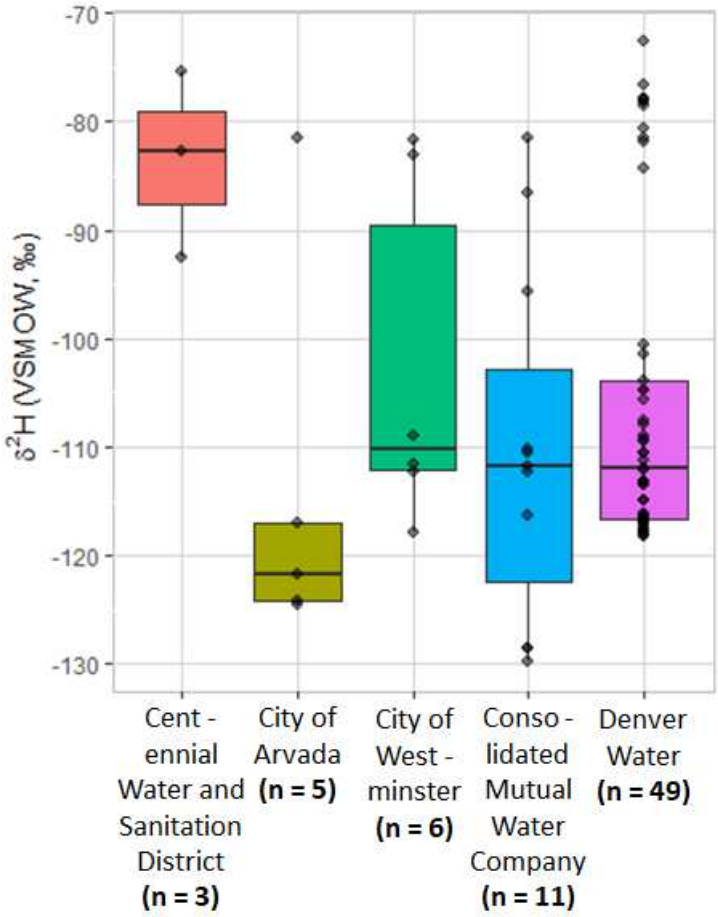

Figure 10. Box plots of the spread of δ^2H over the summer for each water provider

3.5 Flow Contribution Analysis

Six stream samples were chosen for the flow contribution estimation as per the criteria outlined in Methods section 2.5 (chosen samples are indicated by red arrows in figures 8c, 8e, 8i, 8j, and 8m). The precipitation contribution consistently made up less than 40% of the overall streamflow, with the lowest precipitation being 3% of streamflow in Weir Gulch (Table 2, Figure 11b). Tap contributions dominated streamflow on all modeled days with a percent contribution range of 61% - 97% (Table 2, Figure 11a).

The mean daily streamflow depths attributed to tap sources ranged from 0.054 mm - 0.41 mm. High tap water percent contributions (Figure 11a) did not always coincide with high streamflow depths (Figure 11b).

We assumed the total tap contribution was made up of lawn irrigation and infrastructure loss contributions. Because we assumed that all the infrastructure loss reported contributed to baseflow, our infrastructure loss estimates represent the maximum potential contributions to Denver's urban streams. All modeled watersheds had approximately the same area-normalized infrastructure loss depths of 0.05 mm/day since they were all within the Denver Water or Consolidated Mutual Water Company service areas (Tables A11 and A12). However, the proportion of infrastructure loss contributions and LIRF contributions was variable. Separating the estimated contribution from infrastructure loss as part of the tap water contribution, the remaining amount, or 4% - 75% of mean daily flow, was characterized as LIRFs in the urban streams. The associated LIRF flow depths ranged from 3.4×10^{-3} mm - 0.35 mm (Table 2).

Table 2. Summary of contributions to mean daily streamflow for modeled samples. Percent contributions to streamflow are shown below depth contributions and are enclosed in brackets.

Modeled Stream Samples	Precipitation Contribution	Tap Water Contribution	Infrastructure Loss Contribution	Lawn Irrigation Contribution
DUT Sep 30, 2019	0.033 - 0.054 [24% - 39%]	0.084 - 0.11 [61% - 76%]	0.049 [36%]	0.035 - 0.056 [25% - 40%]
HHAR Aug 8, 2019	0.035 - 0.090 [14% - 36%]	0.16 - 0.22 [64% - 86%]	0.052 [21%]	0.11 - 0.17 [44% - 66%]
HHAR Sep 30, 2019	0.075 - 0.15 [16% - 31%]	0.33 - 0.41 [69% - 84%]	0.052 [11%]	0.28 - 0.36 [58% - 74%]
LDA Sep 30, 2019	0.042 - 0.087 [11% - 23%]	0.29 - 0.33 [77% - 89%]	0.052 [14%]	0.23 - 0.28 [63% - 75%]
LDE Sep 30, 2019	0.013 - 0.022 [18% - 29%]	0.054 - 0.062 [71% - 82%]	0.050 [66%]	3.4×10^{-3} - 0.012 [4% - 16%]
WEIR Sep 27, 2019	2.0×10^{-3} - 7.4×10^{-3} [3% - 11%]	0.060 - 0.065 [89% - 97%]	0.052 [77%]	7.7×10^{-3} - 0.013 [11% - 20%]

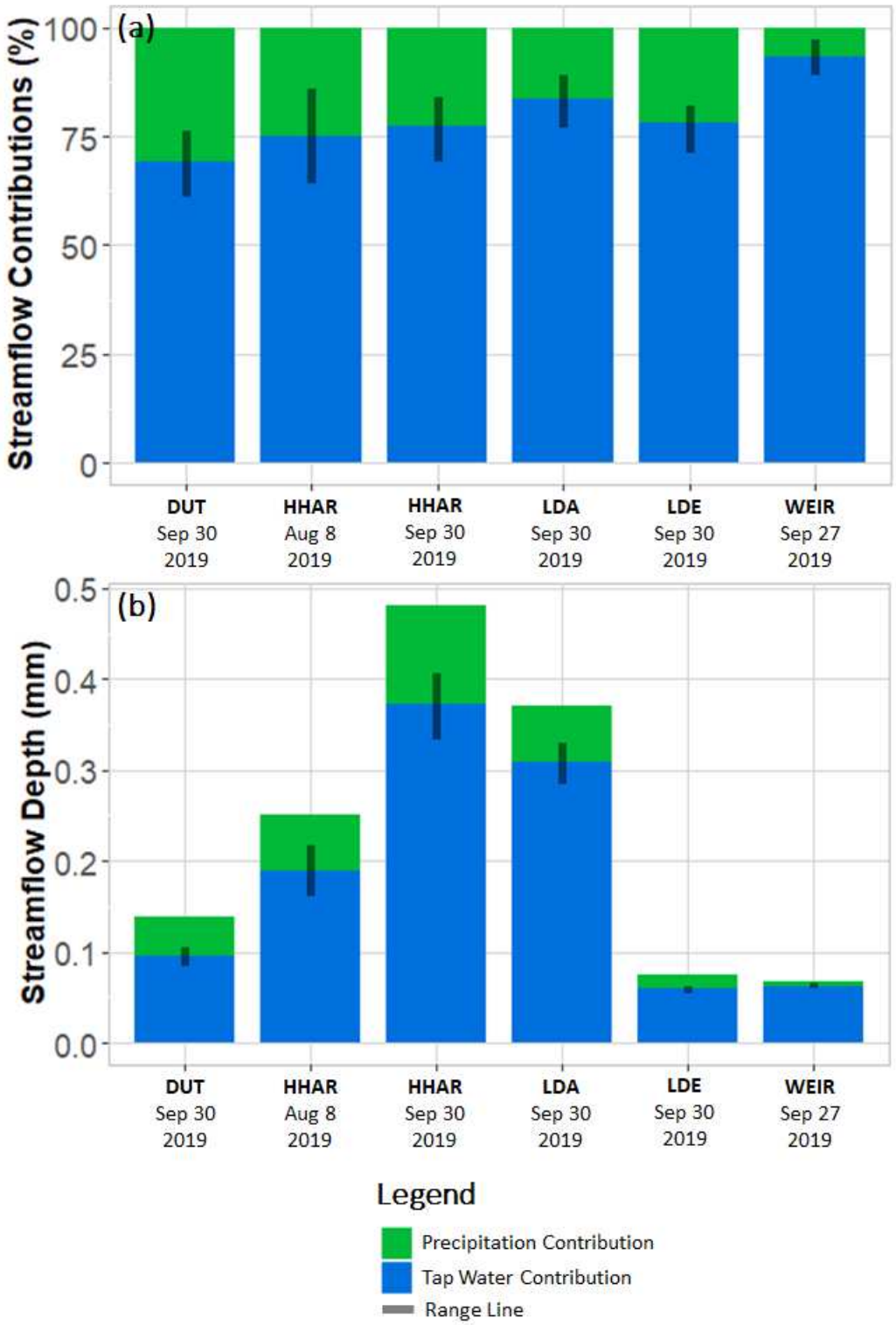

Figure 11. Modeled precipitation, infrastructure loss, and lawn irrigation contributions to streamflow as (a) percentages of total baseflow and (b) streamflow depths (mm) in select streams on specific days. Ranges correspond to maximum and minimum solutions of Equations 3 and 4.

Chapter 4: Discussion

4.1 Tap Contributions to Urban Baseflow

Figure 5 illustrates that there was flow in the urban streams longer than the grassland stream during the 2019 summer. This result is consistent for 2013 - 2019 summer flows (Figure A15). Alteration of the energy gradients driving groundwater flow is one potential cause for this phenomenon. Channel incision and vegetation removal have been suggested as causes of increased groundwater flux into post-development rivers in semi-arid climates (Hibbs *et al.*, 2012). If this were the only cause of increased baseflow in the Denver metropolitan area, we would expect to see higher baseflow in the urban streams than the grassland streams, and both the urban and grassland streams would have similar isotope values as the recent local precipitation isotopes. The grassland stream isotopes did plot with the precipitation isotopes while there was flow (Figures 8n and 8o), but the urban stream values frequently plotted away from the precipitation values, particularly after July 2019 (Figures 8a through 8m). Higher urban streamflow in the Denver metropolitan area cannot be attributed to increased flux of precipitation-recharged groundwater alone.

Urbanization can also elevate streamflow by introducing new sources of water to the hydrologic system, such as tap water. Because none of the studied streams received wastewater effluent, we identified two likely sources of additional water: infrastructure leakage and lawn irrigation. Both infrastructure leakage and lawn irrigation come from tap sources and have been shown to significantly contribute to urban recharge in dry climates (Lerner, 1990). The dominant input of tap water was confirmed by stream isotope values plotting closer to the tap water isotopes than the precipitation isotopes, most notably from July 2019 through September 2019 (Figures 7b, 7c, 8c, 8e, 8i, 8j, and 8m). Our modeled streamflow reflected this tendency, and a majority of streamflow was characterized as sourced from tap water (Table 2, Figure 11a). Eleven out of 13 urban flows had streamflow within the modeled tap daily flow depth range (0.054 mm - 0.41 mm) at the 10th percentile (Figure 5). This shows

that even the lower urban flows experienced during summer 2019 were generally within the observed tap contribution range. Elevated baseflow in the Denver metropolitan area can be attributed to tap water sources.

4.2 Infrastructure Leakage and Lawn Irrigation Contributions to Urban Baseflow

Our estimates found that both infrastructure leakage and lawn irrigation inputs were present in Denver's urban streams, and the relative contributions from each source varied by watershed. Approximately 7.2% of Denver's annual water distribution was considered "loss" in the 2018 Denver Water report (Colorado Water Conservation Board, 2018). A 7.2% loss percentage is comparable to other semi-arid cities in the United States such as Los Angeles (7% - 9%) (Garcia-Fresca & Sharp, 2005). The infrastructure loss flow rate for the modeled watersheds, 0.05 mm/day, was low in comparison to reported infrastructure loss rates for humid subtropical cities in the United States. Studies conducted in Baltimore, Maryland, USA and Austin, Texas, USA reported area-normalized infrastructure loss estimates of 0.43 mm/day and a range of 0.07 mm/day - 0.32 mm/day, respectively (Bhaskar & Welty, 2012; Garcia-Fresca & Sharp, 2005). Loss included unauthorized use and inaccuracies in metering and leakage, whereas only leakage would contribute to tap water contributions to urban streams (Karamouz *et al*., 2010). We assumed that 100% of the infrastructure loss reached the urban stream, neglecting ET use, so our loss estimates were conservatively high. The daily flow depth range for LIRFs (3.4×10^{-3} mm - 0.28 mm) spanned nearly two orders of magnitude (Table 2). The Denver lawn irrigation range coincided with the reported Baltimore lawn irrigation flow depth, 0.068 mm/day, and was low in comparison to the 2.2 mm/day irrigation application estimates in nearby Aurora, Colorado (Bhaskar & Welty, 2012; Gage & Cooper, 2015). Some water applied for irrigation purposes will be taken up by plants, so the lawn irrigation contribution to the streams should be lower than the application rate. Using the Aurora lawn irrigation application rate, we estimated that ~0% to 12% of irrigation water will flow to an urban stream in the Denver metropolitan area. These estimates represented the lower bounds of expected lawn irrigation contributions since our lawn irrigation contributions were inversely related to infrastructure loss contributions in our model and our loss estimates were at their maximums.

4.3. Assumptions and Limitations

One of our driving motivations for this study was lack of data on contributors to streamflow and water-stable isotope trends in the Denver metropolitan area. Unfortunately, this also served as an overarching limitation to our study. Because we did not have sufficient historical water table, precipitation, tap, or stream data, we could not compare our results from 2019 to results from previous years and assumptions needed to be made in the absence of information.

The non-tap (i.e. no irrigation or infrastructure leakage) groundwater component was difficult to account for in our watersheds. We did not have access to wells that were in areas that did not receive irrigation to characterize groundwater from precipitation-induced recharge, as much of the area either received lawn or agricultural irrigation. The contribution and timing of recharge from precipitation in this water-limited environment requires greater research. A recent USGS report contained isotope data on Denver's groundwater, but focus was placed on deep groundwater instead of local water tables (Musgrove *et al*., 2014). Two water table isotope data points were included in the report, but the points were taken in an urban setting and could have received lawn irrigation as well. None of our watersheds contained groundwater upwelling points or were connected to the South Platte alluvial aquifer according to Denver's official "Groundwater Seeps" dataset, so we were not concerned with deep groundwater inputs to our streams (City and County of Denver, 2019). Because of this, we assumed that an average precipitation value over a two-week period served as a reasonable proxy for the non-tap component contributing to streamflow. If groundwater contributions to the stream were mixed with longer travel times, the isotopic values may resemble Denver's mean annual precipitation isotope values (δ^2H = -82.8‰, $\delta^{18}O$ = -11.2‰) (Bowen, 2020; Bowen *et al*., 2005; International Atomic Energy Agency, 2015; Welker, 2000). If this were the case, stream isotope values occurring in July 2019 and August 2019 would be higher than both the groundwater and tap end members (Figures 8a through 8m). Late August 2019 and September 2019 values for modeled watersheds would still be constrained between tap and precipitation-recharged groundwater, but the tap proportions would decrease (Figures 8c, 8e, 8i, 8j and 8m).

Recent precipitation isotope data was limited in the Denver metropolitan area, so we decided to deploy two precipitation samplers for our study. However, we cannot argue that we completely captured the behavior of Denver's precipitation isotopes due to the precipitation sampling sites being located in the northernmost portion of the study area (Figure 2). Because our study area was large, it was not uncommon for storms to occur in the southern region of the Denver metropolitan area and not in the northern region, and those storms were not included in our precipitation sampling. Our ability to describe the isotopic behavior of Denver's precipitation was also limited by taking composite monthly samples. This sampling design was chosen to help account for isotopic changes within individual storms, but the tradeoff was fewer samples were yielded because of it. When comparing our precipitation results to mean monthly precipitation values (Bowen, 2020; Bowen *et al*., 2005; International Atomic Energy Agency, 2015; Welker, 2000) our measured precipitation isotopes were low from April 2019 - June 2019 and high from July - 2019 September 2019 (Figures 6, A16 and A17). The large deviation of our measured precipitation points from the GMWL and LMWL could indicate that unwanted evaporation was occurring within our July 2019 – September 2019 samples (Figure 6). This was despite the precipitation isotope samplers being designed to prevent post-collection evaporation (Palmex Ltd., 2019).

We did not capture the tap water variation for many water providers throughout the summer, with most of our tap data being taken from Denver Water until August 2019. The isotopic differences between the water providers and temporal variations were larger than anticipated, and we did create a new sampling strategy to better capture this variation in August. Limited sampling decreases our ability to draw conclusions about trends for specific water providers. We also learned that a water entity in our study area, Consolidated Mutual Water Company, was not a part of the Denver Water service area by our definition. Consolidated Mutual Water Company is on Denver Water's official distributor list, but we did not learn until the end of July that Consolidated Mutual Water Company combines Denver Water's water with water from other sources (Denver Water, 2020). The Denver Water distributor list does not imply each water entity buys water exclusively from Denver Water. It did not seem appropriate to model many

of our watersheds due to lack of tap data, so all modeled watersheds (Figure 11) were predominantly within the Denver Water service area boundary.

Because sampling tap sources (i.e., reservoirs) can be a security risk, we needed to make assumptions about our tap samples. We were unable to get isotope data directly from water providers, so we assumed that water taken from taps had not undergone any isotopic fractionation en route to the taps. It was not feasible to sample sprinklers and leaking pipes directly, and we assumed that both of these sources had the same isotopic signature as tap samples supplied by the common water provider. Some of the parks in the Denver metropolitan area use reclaimed tap water for irrigation, and we assumed that reclaimed water looks the same isotopically as the tap water we measured. We assumed no isotopic fractionation occurred between the sprinkler or leakage point and the urban stream. If evaporative fractionation occurred, we would expect isotopic values associated with tap contributions to be higher than our measured tap values. This could potentially prevent us from constraining our stream samples between two end-members as the stream isotopic values were often just above the tap values (Figures 8b through 8m). We also assumed that all other potential sources of tap water, such as soil-wetting for land development, were negligible.

4.4 Implications and Future Work

There are substantial contributions from tap sources to late summer (August - September) baseflow in the Denver Metropolitan Area. The prevalence of LIRFs in Denver streams varies between watersheds, and the largest lawn irrigation contributions occur in streams with the highest area-normalized mean daily streamflow depths. Increased baseflow can affect stream characteristics such as bank stability, stream health, and stream/riparian ecology. Higher baseflow can increase channel erosion and elevate streamflow levels during storm events. Depending on the water quality characteristics of baseflow compared to stormflow, stream water quality may be degraded or improved by greater baseflow. Water quality may be deteriorated by the introduction of fertilizers from lawn irrigation or chlorine from treated water. However, water quality may be improved if the increased flows diluted the concentration of incoming stormflow contaminants, with resulting effects on abundances of in-stream or near-stream biota.

Tap water contributing most of the water to urban streams on sunny days may seem inherently problematic from a water use efficiency perspective, since this water was applied for landscape plant growth. From a water rights perspective, transbasin tap water that returns to urban streams can be claimed as a return flow credit that allows municipalities to withdraw the equivalent amount upstream. Many municipalities claim 15% of the lawn irrigation application rate as a return flow credit (Oad & DiSpigno, 1997). Our maximum estimate of LIRFs to urban streams was 12% of an assumed irrigation 600 mm application rate based on Aurora, Colorado (Gage & Cooper, 2015), which suggests that consumers in the Denver metropolitan area may not always be contributing 15% as LIRF.

Our research spanned a single summer, so it is unclear what the broader patterns are over multiple years with variable climate and over more watersheds. However, we have enough evidence to warrant further investigations into the role that tap water and lawn irrigation play in semi-arid, urban streams. Water-stable isotope analysis proved effective at differentiating between tap water and local precipitation signals, so we recommend conducting more sampling over multiple years and beyond the summer season to better understand how the isotopes change over time. Increasing the number of precipitation samplers or increasing the distance between them would help better capture the spatial variation of precipitation isotopes throughout the Denver metropolitan area. Installation of local groundwater isotope sampling stations both in urbanized and grassland watersheds would help reduce the number of assumptions needed.

Chapter 5: Conclusions

Semi-arid and arid cities need to understand their local hydrology to ensure precious water resources are conserved and managed effectively. The impact of lawn irrigation on urban streamflow is not well understood, but the little research that has been done suggests that it may play an important role in the semi-arid, urban water cycle. We aimed to increase understanding of Denver's urban water cycle by estimating the contributions made by (1) tap water and (2) lawn irrigation to summertime baseflow with water-stable isotope (δ^2H and δ^{18}O) analysis. Urban stream, grassland stream, tap, and precipitation isotope samples were taken and analyzed in September 2018 as well as from March 2019 through September 2019 (Figure 7). A two end-member mixing model was used to estimate the contributions of tap water and meteoric water to urban baseflow based on the δ^2H and δ^{18}O values from select days. The lawn irrigation component to baseflow was calculated by subtracting reported water distribution infrastructure losses from the overall tap contribution to baseflow. The answers to our research questions are stated below:

(1) *How much of Denver's summertime baseflow comes from tap water sources?*

We found that tap water made up the majority (61% - 97%) of urban baseflow in all modeled days and the contribution depth range was 0.054 mm - 0.41 mm (Table 2, Figure 11a).

(2) *How much of the tap water contribution can be attributed to lawn irrigation compared to other sources of tap water?*

Lawn irrigation comprised 4% - 75% of the flow in our watersheds and contributed flow depths ranging from 3.4 x 10^{-3} mm to 0.35 mm (Table 2). This is a conservative estimate as we assumed all infrastructure loss, the other main pathway for tap water to become streamflow, becomes baseflow.

Useful areas for future work include characterizing the isotopic behavior of Denver's baseflow over multiple years to better understand the long-term effects urbanization has had on Denver's hydrology.

References

ARUP. (2018). *Cities Alive: Rethinking Cities in Arid Environments*. Retrieved from https://www.arup.com/perspectives/publications/research/section/cities-alive-cities-in-arid-environments

Bhaskar, A. S., & Welty, C. (2012). Water Balances along an Urban-to-Rural Gradient of Metropolitan Baltimore, 2001-2009. *Environmental & Engineering Geoscience*, *18*(1), 37–50. doi: 10.2113/gseegeosci.18.1.37

Bhaskar, A. S., Beesley, L., Burns, M. J., Fletcher, T. D., Hamel, P., Oldham, C. E., & Roy, A. H. (2016). Will it Rise or Will it Fall? Managing the Complex Effects of Urbanization on Base Flow. *Freshwater Science*, *35*(1), 293–310. doi: 10.1086/685084

Bowen, G. J., Wassenaar, L. I., & Hobson, K. A. (2005). Global Application of Stable Hydrogen and Oxygen Isotopes to Wildlife Forensics. *Oecologia*, *143*(3), 337–348. doi: 10.1007/s00442-004-1813-y

Bowen, G. J. (2020) Gridded Maps of the Isotopic Composition of Meteoric Waters. Retrieved from http://www.waterisotopes.org

Catena Analytics. (2019). eRAMS GIS Tools. Retrieved from https://erams.com/catena/gis/erams-tools/

Centennial Water and Sanitation District. (2012). Highlands Ranch Water Supply Fact Sheet. Retrieved from https://www.centennialwater.org/water-wastewater-services/water/

City and County of Denver. (2019). Open Data Catalog. Retrieved from https://www.denvergov.org/opendata

City of Arvada. (2005). Water Sources, Treatment, and Distribution. Retrieved from https://www.arvada.org/residents/services-and-sustainability/water-sourcestreatment-and-distribution

City of Golden. (2020). Water Supply. Retrieved from https://www.cityofgolden.net/government/departments-divisions/water/water-supply/

City of Westminster. (2017). Where Does Your Drinking Water Come From? Retrieved from https://www.cityofwestminster.us/News/where-does-your-drinking-water-come-from

Coles, J.F., McMahon, G., Bell, A.H., Brown, L.R., Fitzpatrick, F.A., Scudder Eikenberry, B.C., Woodside, M.D., Cuffney, T.F., Bryant, W.L., Cappiella, K., Fraley-McNeal, L., & Stack, W.P. (2012). *Effects of Urban Development on Stream Ecosystems in Nine Metropolitan Study Areas Across the United States* (USGS Circular 1373). Retrieved from https://pubs.usgs.gov/circ/1373/pdf/Circular1373.pdf

Colorado Water Conservation Board. (2018). Water Efficiency Data Portal. Retrieved from http://www.cowaterefficiency.com/

Consolidated Mutual Water Company. (2019). Service Area Map. Retrieved from https://www.cmwc.net/about-us/service-area-map/

Consolidated Mutual Water Company. (2020). Water Sources and Storage Levels. Retrieved from https://www.cmwc.net/your-water/sources-storage-levels/

Cook, C. S., Erkkila, B. R., Chakraborty, S., Tipple, B. J., Cerling, T. E., & Ehleringer, J. R. (2018). *Stable Isotope Biogeochemistry and Ecology: Laboratory Manual*. Salt Lake City, UT: University of Utah.

Craig, H. (1961). Isotopic Variations in Meteoric Waters. *Science*, 133(3465), 1702–1703. doi: 10.1126/science.133.3465.1702

Denver Water. (2020). Distributors. Retrieved from https://www.denverwater.org/about-us/how-we-operate/service-area/distributors

DeOreo, W. B., Mayer, P. W., Dziegielewski, B., & Kiefer, J. (2016). *Residential End Uses of Water, Version 2: Executive Report*. Denver, CO: Water Research Foundation. Retrieved from https://www.waterrf.org/research/projects/residential-end-uses-water-version-2

Droplet Clipart Water Sprinkle [PNG Image]. (2020). Retrieved from https://www.ya-webdesign.com/explore/droplet-clipart-water-sprinkle/

Dyson, K., Ziter, C., Fuentes, T. L., & Patterson, M. S. (2019). Conducting Urban Ecology Research on Private Property: Advice for New Urban Ecologists. *Journal of Urban Ecology*, 5(1). doi: 10.1093/jue/juz001

Ehleringer, J. R., Barnette, J. E., Jameel, Y., Tipple, B. J., & Bowen, G. J. (2016). Urban Water – A New Frontier in Isotope Hydrology. *Isotopes in Environmental and Health Studies*, 52(4-5), 477–486. doi: 10.1080/10256016.2016.1171217

Gage, E., & Cooper, D. J. (2015). The Influence of Land Cover, Vertical Structure, and Socioeconomic Factors on Outdoor Water Use in a Western US City. *Water Resources Management*, *29*(10), 3877–3890. doi: 10.1007/s11269-015-1034-7

Garcia-Fresca, B., & Sharp, J. M. (2005). Hydrogeologic Considerations of Urban Development: Urban-Induced Recharge. *Humans as Geologic Agents*. doi: 10.1130/2005.4016(11)

Gleick, P. H. (2010). Roadmap for Sustainable Water Resources in Southwestern North America. *Proceedings of the National Academy of Sciences*, 107(50), 21300–21305. doi: 10.1073/pnas.1005473107

Global Network of Isotopes in Precipitation & International Atomic Energy Agency. (2014). IAEA/GNIP Precipitation Sampling Guide. Retrieved from http://www-naweb.iaea.org/napc/ih/documents/other/gnip_manual_v2.02_en_hq.pdf

Gober, P., Quay, R., & Larson, K. L. (2015). Outdoor Water Use as an Adaptation Problem: Insights from North American Cities. *Water Resources Management*, *30*(3), 899–912. doi: 10.1007/s11269-015-1205-6

Green Grass on a Transparent Background [PNG Image]. (2020). Retrieved from https://www.pixy.org/650056/

Harvey, F. E. (2005). Stable Hydrogen And Oxygen Isotope Composition Of Precipitation In Northeastern Colorado. *Journal of the American Water Resources Association*, 41(2), 447–460. doi: 10.1111/j.1752-1688.2005.tb03748.x

Hibbs, B. J., Hu, W., & Ridgway, R. (2012). Origin of Stream Flows at the Wildlands-Urban Interface, Santa Monica Mountains, California, U.S.A. *Environmental & Engineering Geoscience*, 18(1), 51–64. doi: 10.2113/gseegeosci.18.1.51

Hopkins, K. G., Morse, N. B., Bain, D. J., Bettez, N. D., Grimm, N. B., Morse, J. L., Palta, M. M., Shuster, W. D., Bratt, A. R., Suchy, A. K. (2015). Assessment of Regional Variation in Streamflow Responses to Urbanization and the Persistence of Physiography. *Environmental Science & Technology*, *49*(5), 2724–2732. doi: 10.1021/es505389y

International Atomic Energy Agency. (2015). WISER – Water Isotope System for data analysis, visualization and Electronic Retrieval. Retrieved from https://nucleus.iaea.org/

Jefferson, A. J., Bell, C. D., Clinton, S. M., & Mcmillan, S. K. (2015). Application of Isotope Hydrograph Separation to Understand Contributions of Stormwater Control Measures to Urban Headwater Streams. *Hydrological Processes*, 29(25), 5290–5306. doi: 10.1002/hyp.10680

Karamouz, M., Moridi, A., & Nazif, S. (2010). *Urban Water Engineering and Management*. Boca Raton, FL: CRC Press/Taylor & Francis.

Kendall, C., & McDonnell, J. J. (1998). *Isotope Tracers in Catchment Hydrology*. Amsterdam, NL: Elsevier.

Leonard Rice Engineers, Inc. (2015). Colorado Water Entities. Retrieved from http://www.lre-projects.com/ColoradoWaterEntities/

Lerner, D. N. (1990). Groundwater Recharge in Urban Areas. *Atmospheric Environment. Part B. Urban Atmosphere*, *24*(1), 29–33. doi: 10.1016/0957-1272(90)90006-g

Manago, K. F., & Hogue, T. S. (2017). Urban Streamflow Response to Imported Water and Water Conservation Policies in Los Angeles, California. *JAWRA Journal of the American Water Resources Association*, *53*(3), 626–640. doi: 10.1111/1752-1688.12515

Musgrove, M., Beck, J.A., Paschke, S.S., Bauch, N.J., and Mashburn, S.L. (2014). *Quality of Groundwater in the Denver Basin Aquifer System, Colorado, 2003–5* (USGS report 2014–5051). Retrieved from https://pubs.usgs.gov/sir/2014/5051/

National Oceanic and Atmospheric Administration. (2020). Climate Denver - Colorado. Retrieved from https://www.usclimatedata.com/climate/denver/colorado/united-states/usco0105

Navarro Research and Engineering, Inc. (2019). Mean Daily Discharge from Rocky Flats WOMPOC Site for the 2019 Calendar Year [Microsoft Excel Spreadsheet].

Oad, R., & DiSpigno, M. (1997). Water Rights to Return Flow from Urban Landscape Irrigation. *Journal of Irrigation and Drainage Engineering*, *123*(4), 293–299. doi: 10.1061/(asce)0733-9437(1997)123:4(293)

Palmex Ltd. (2019). Palmex Rain Sampler RS1. Retrieved from http://www.rainsampler.com/portfolio-page/rain-sampler-rs1/

Roots Black and White PNG Icon. (2018). Retrieved from https://www.iconspng.com/image/131611/roots-black-and-white

Simpson, H. J., & Herczeg, A. L. (1991). Stable Isotopes as an Indicator of Evaporation in the River Murray, Australia. *Water Resources Research*, *27*(8), 1925–1935. doi: 10.1029/91wr00941

SIRFER. (2020). Oxygen and Hydrogen Analysis of Water. Retrieved from https://sirfer.utah.edu/oxygen-and-hydrogen-analysis-of-water.html

Theriault, A. (2020). Gravel Brown Stone Texture Dirt [JPG Image]. Retrieved from https://www.pixy.org/69527/

United States Census Bureau. (2019). Annual Estimates of the Resident Population for Counties: April 1, 2010 to July 1, 2018. Retrieved from https://factfinder.census.gov

United States Census Bureau. (1996). Population of States and Counties of the United States: 1790 to 1990. Retrieved from https://factfinder.census.gov

United States Department of Agriculture. (2018). Natural Resources Conservation Service: Geospatial Data Gatway. Retrieved from https://datagateway.nrcs.usda.gov/

United States Geological Survey. (2019). National Water Information System: Web Interface. Retrieved from https://waterdata.usgs.gov/co/nwis/rt

United States Geological Survey. (2020). StreamStats: Streamflow Statistics and Spatial Analysis Tools for Water-Resources Applications. Retrieved from https://www.streamstats.usgs.gov/ss/

University of Utah. (2019). Waterisotopes Database. Query: Country = US, State/Province = CO, Type = Tap, Project ID = 00099 and 00225. Retrieved from http://wateriso.utah.edu/waterisotopes/index.html

Welker, J. M. (2000). Isotopic ($\delta^{18}O$) Characteristics of Weekly Precipitation Collected Across the USA: an Initial Analysis with Application to Water Source Studies. *Hydrological Processes*, *14*(8), 1449–1464. doi: 10.1002/1099-1085(20000615)14:8<1449::aid-hyp993>3.0.co;2-7

Appendix

Key to water provider abbreviations used in this document:
ARV refers to City of Arvada
CENT refers to Centennial Water and Sanitation District
CMWC refers to Consolidated Mutual Water Company
DEN refers to Denver Water
GOLD refers to City of Golden
WEST refers to City of Westminster

Table A1. Isotope sample data. "Abbr." refers to abbreviations for stream, precipitation, or tap sampling locations.

Date	Month - Year	Month Number	Day of Year	Time (MST)	Abbr.	δ^2H	$\delta^{18}O$	Notes
2018-09-10	Sep-18	9	253	10:35	LDW	-102.5	-13.0	Mean, Improper Crimping
2018-09-10	Sep-18	9	253	11:08	LENA	-95.5	-12.4	Mean, Improper Crimping
2018-09-10	Sep-18	9	253	11:25	TW	-110.1	-14.4	Mean, Improper Crimping
2018-09-10	Sep-18	9	253	12:00	WEIR	-103.6	-13.0	Mean, Improper Crimping
2018-09-10	Sep-18	9	253	12:15	DRY	-93.0	-11.9	Mean, Improper Crimping
2018-09-10	Sep-18	9	253	12:24	LAKE	-99.4	-12.7	Mean, Improper Crimping
2018-09-14	Sep-18	9	257	11:15	HHAR	-97.7	-11.8	Improper Crimping
2018-09-14	Sep-18	9	257	11:38	LDE	-94.0	-11.6	Improper Crimping
2018-09-14	Sep-18	9	257	12:07	LEE	-91.6	-11.2	Improper Crimping, Barely Flowing (Sampled from puddle)
2018-09-14	Sep-18	9	257	12:27	NTW	-112.0	-14.3	Improper Crimping
2018-09-14	Sep-18	9	257	13:10	DUT	-81.8	-10.1	Improper Crimping
2018-09-14	Sep-18	9	257	13:50	BIG	-97.7	-12.5	Improper Crimping
2018-09-14	Sep-18	9	257	14:15	LDA	-103.1	-12.9	Improper Crimping
2019-03-23	Mar-19	3	82	12:22	STW	-104.7	-13.3	NA

2019-04-13	Apr-19	3	103	12:33	GABE1	-117.2	-15.3	Gabe Bowen - Project ID: 00099
2019-04-18	Apr-19	4	108	7:18:30	LENA	-104.5	-13.4	NA
2019-04-18	Apr-19	4	108	7:41	WEIR	-106.7	-13.5	NA
2019-04-18	Apr-19	4	108	7:56:30	DRY	-107.5	-13.8	NA
2019-04-18	Apr-19	4	108	8:08:30	LAKE	-110.2	-14.3	NA
2019-04-18	Apr-19	4	108	8:32	PHP	-98	-13.5	NA
2019-04-18	Apr-19	4	108	8:59:30	LDF	-109.9	-13.9	NA
2019-04-18	Apr-19	4	108	9:16:30	LDW	-108.9	-13.9	NA
2019-04-18	Apr-19	4	108	9:34	7TW	-108.9	-13.7	NA
2019-04-25	Apr-19	4	115	6:41:15	LDA	-102.7	-13.1	NA
2019-04-25	Apr-19	4	115	7:00:45	BIG	-101.5	-12.9	NA
2019-04-25	Apr-19	4	115	7:31:15	DUT	-91.7	-10.7	NA
2019-04-25	Apr-19	4	115	7:51:45	LEE	-96	-12.1	NA
2019-04-25	Apr-19	4	115	8:11	LDE	-98.6	-12.5	NA
2019-04-25	Apr-19	4	115	8:32:45	HCOL	-104.5	-13.3	NA
2019-04-25	Apr-19	4	115	8:45:45	HHAR	-98.1	-12.1	NA
2019-04-25	Apr-19	4	115	8:55	CTW	-100.6	-12.2	NA
2019-05-02	May-19	5	122	7:20:00	SWOM	-97.4	-11.8	NA
2019-05-02	May-19	5	122	7:38:00	WOM	-104.9	-13.4	NA
2019-05-13	May-19	5	133	8:26:08	SWOM	-95.7	-11.5	NA
2019-05-13	May-19	5	133	8:44:41	WOM	-103.1	-13.4	NA
2019-05-13	May-19	5	133	9:51:24	LENA	-98.3	-12.5	NA
2019-05-13	May-19	5	133	10:11:04	WEIR	-106.3	-13.6	NA
2019-05-13	May-19	5	133	10:21:20	DRY	-118.2	-15.5	NA

2019-05-13	May-19	5	133	10:30:11	LAKE	-115.9	-15.2	NA
2019-05-13	May-19	5	133	11:35	STTW	-101.5	-12.5	NA
2019-05-13	May-19	5	133	12:14:05	LDF	-95.1	-11	NA
2019-05-13	May-19	5	133	12:27:00	LDW	-97.6	-11.6	NA
2019-05-24	May-19	5	144	9:40	PHP	-105.9	-14.6	Sampler Tipped Over
2019-05-24	May-19	5	144	12:00:15	SWOM	-96.2	-11.7	NA
2019-05-24	May-19	5	144	12:16:00	WOM	-107.2	-13.9	NA
2019-05-31	May-19	5	151	9:45	LDA	-103.8	-13.2	NA
2019-05-31	May-19	5	151	10:14	BIG	-102.5	-13.2	NA
2019-05-31	May-19	5	151	10:48	DUT	-97.9	-12.3	NA
2019-05-31	May-19	5	151	11:15	LEE	-101.4	-12.9	NA
2019-05-31	May-19	5	151	11:40	LDE	-102	-12.9	NA
2019-05-31	May-19	5	151	11:52	HHAR	-99.6	-12.3	NA
2019-05-31	May-19	5	151	12:07	HCOL	-101.5	-13.1	NA
2019-05-31	May-19	5	151	12:24	NGTW	-103.9	-12.9	NA
2019-06-07	Jun-19	6	158	8:15	SWOM	-85.9	-10.5	Estimated Time (Not Recorded), Not Baseflow
2019-06-07	Jun-19	6	158	8:32	WOM	-90	-11.5	Not Baseflow
2019-06-12	Jun-19	6	163	9:31	WOM	-96	-12	NA
2019-06-12	Jun-19	6	163	11:17	LAKE	-117.3	-15.3	NA
2019-06-12	Jun-19	6	163	12:26	MDTW	-104.7	-13.1	NA
2019-06-12	Jun-19	6	163	13:10	BIG	-99.1	-12.6	Estimated Time (Not Recorded)
2019-06-20	Jun-19	6	171	13:58	WOM	-98.2	-12.4	NA
2019-06-27	Jun-19	6	178	9:31	TLR	-72	-9.8	Gooey, Lost Part of Sample (Opened in cooler)

2019-06-27	Jun-19	6	178	10:28	LENA	-99	-12.8	NA
2019-06-27	Jun-19	6	178	10:50	WEIR	-114.8	-14.9	NA
2019-06-27	Jun-19	6	178	11:02	DRY	-124.8	-16.5	NA
2019-06-27	Jun-19	6	178	11:10	LAKE	-117.5	-15.5	NA
2019-06-27	Jun-19	6	178	11:53	CKTW	-116.1	-15	NA
2019-06-27	Jun-19	6	178	12:07	PHP	-81.6	-11.1	NA
2019-06-27	Jun-19	6	178	12:30	LDF	-106.4	-13.6	NA
2019-06-27	Jun-19	6	178	12:44	LDW	-114.8	-14.9	NA
2019-07-11	Jul-19	7	192	10:06	LDA	-90.9	-11.3	NA
2019-07-11	Jul-19	7	192	10:33	BIG	-88.7	-11.1	NA
2019-07-11	Jul-19	7	192	11:10	DUT	-80.4	-10.2	NA
2019-07-11	Jul-19	7	192	12:30	BBTW	-78.6	-10	NA
2019-07-11	Jul-19	7	192	12:46	LEE	-72.1	-9	NA
2019-07-11	Jul-19	7	192	13:09	LDE	-72.5	-9.1	NA
2019-07-11	Jul-19	7	192	13:24	HHAR	-67.5	-7.5	NA
2019-07-11	Jul-19	7	192	13:35	HCOL	-72.2	-8.6	NA
2019-07-22	Jul-19	7	203	9:26	LDW	-83.2	-10.7	NA
2019-07-22	Jul-19	7	203	11:13	LAKE	-69.8	-9.5	NA
2019-07-22	Jul-19	7	203	13:15	BIG	-79.7	-10.1	NA
2019-07-22	Jul-19	7	203	15:35	SAF	-83	-10	NA
2019-07-25	Jul-19	7	206	8:32	LDW	-90	-11.6	NA
2019-07-25	Jul-19	7	206	8:48	LDF	-84.9	-10.8	NA
2019-07-25	Jul-19	7	206	9:13	PHP	-41.6	-3.7	NA
2019-07-25	Jul-19	7	206	9:31	LAKE	-104.2	-13.9	NA
2019-07-25	Jul-19	7	206	9:41	DRY	-88.9	-11.5	NA

2019-07-25	Jul-19	7	206	9:53	WEIR	-70.4	-8.4	NA
2019-07-25	Jul-19	7	206	10:05	DINO	-80.6	-10.3	NA
2019-07-25	Jul-19	7	206	10:30	LENA	-80.5	-10.4	NA
2019-07-25	Jul-19	7	206	11:01	TLR	-44.9	-5.3	NA
2019-08-01	Aug-19	8	213	9:08	LDA	-69.7	-8.1	NA
2019-08-01	Aug-19	8	213	9:36	BIG	-69.5	-8.8	NA
2019-08-01	Aug-19	8	213	10:08	LEE	-60.5	-7.4	NA
2019-08-01	Aug-19	8	213	10:32	CIRK	-81.5	-10.3	NA
2019-08-01	Aug-19	8	213	10:57	LDE	-71.1	-8.7	NA
2019-08-01	Aug-19	8	213	11:09	HHAR	-65.8	-8.2	NA
2019-08-01	Aug-19	8	213	11:21	HCOL	-58.3	-7.1	NA
2019-08-05	Aug-19	8	217	5:42	KSO	-81.5	-10.5	NA
2019-08-05	Aug-19	8	217	5:57	LDW	-93.1	-11.9	NA
2019-08-05	Aug-19	8	217	6:07	7TW	-81.7	-10.4	NA
2019-08-05	Aug-19	8	217	6:15	LDF	-76.9	-9.8	NA
2019-08-05	Aug-19	8	217	6:38	LAKE	-79.6	-10.2	NA
2019-08-05	Aug-19	8	217	6:46	DRY	-73.6	-8.7	NA
2019-08-05	Aug-19	8	217	6:57	WEIR	-84	-10.1	NA
2019-08-05	Aug-19	8	217	7:13	TAR	-84.3	-10.5	Small air bubble
2019-08-05	Aug-19	8	217	7:23	WAL	-95.6	-12.3	NA
2019-08-05	Aug-19	8	217	7:32	WAL2	-86.5	-11.2	NA
2019-08-05	Aug-19	8	217	7:43	LENA	-83.2	-10.3	NA
2019-08-05	Aug-19	8	217	7:55	SHEL	-81.5	-10.5	NA
2019-08-08	Aug-19	8	220	7:46	SAF2	-76.6	-9.7	NA
2019-08-08	Aug-19	8	220	8:09	PAN	-77.8	-9.9	NA

2019-08-08	Aug-19	8	220	8:35	BIG	-75.9	-9.6	NA
2019-08-08	Aug-19	8	220	9:01	WAG	-75.3	-9.5	NA
2019-08-08	Aug-19	8	220	9:24	SAF3	-78.2	-9.8	NA
2019-08-08	Aug-19	8	220	9:46	DUT	-82.7	-10.7	NA
2019-08-08	Aug-19	8	220	10:05	TAR2	-78	-9.7	Small air bubble
2019-08-08	Aug-19	8	220	10:38	HHAR	-69.9	-8.3	NA
2019-08-08	Aug-19	8	220	10:46	CTW	-72.6	-9.1	NA
2019-08-08	Aug-19	8	220	11:07	KSO2	-81.9	-10.3	NA
2019-08-26	Aug-19	8	238	8:28	LDW	-100.3	-12.5	Small air bubble
2019-08-26	Aug-19	8	238	8:44	LDF	-93.5	-11.8	NA
2019-08-26	Aug-19	8	238	9:09	PHP	-24.4	-2.5	Small air bubble
2019-08-26	Aug-19	8	238	9:35	LAKE	-108.6	-14.2	NA
2019-08-26	Aug-19	8	238	9:45	DRY	-111.5	-14.7	NA
2019-08-26	Aug-19	8	238	9:59	WEIR	-104.3	-13.3	NA
2019-08-26	Aug-19	8	238	10:20	HHAR	-85.8	-10.1	Small air bubble
2019-08-26	Aug-19	8	238	11:07	LENA	-96.9	-12.5	NA
2019-08-26	Aug-19	8	238	11:40	TW	-112.3	-14.8	NA
2019-08-26	Aug-19	8	238	12:14	TLR	-21.6	-0.7	Small air bubble
2019-09-04	Sep-19	9	247	9:21	LDA	-100.2	-12.6	NA
2019-09-04	Sep-19	9	247	9:35	MD2	-109.3	-13.8	NA
2019-09-04	Sep-19	9	247	10:01	BIG	-93.1	-11.7	NA
2019-09-04	Sep-19	9	247	10:32	LEE	-87.3	-10.4	NA
2019-09-04	Sep-19	9	247	10:51	DUT	-91.3	-11.1	NA
2019-09-04	Sep-19	9	247	11:10	LDE	-88.7	-10.7	Small air bubble
2019-09-04	Sep-19	9	247	11:21	HHAR	-93.7	-11.5	NA

2019-09-04	Sep-19	9	247	11:30	HCOL	-99.4	-12.3	NA
2019-09-13	Sep-19	9	256	11:20	LENA	-95.2	-12.1	NA
2019-09-13	Sep-19	9	256	11:46	WEIR	-104.4	-13.5	NA
2019-09-13	Sep-19	9	256	11:55	DRY	-108.1	-14.1	Small air bubble
2019-09-13	Sep-19	9	256	12:03	LAKE	-104.6	-13.5	Large air bubble
2019-09-13	Sep-19	9	256	12:27	LDF	-82.1	-10.7	NA
2019-09-13	Sep-19	9	256	12:37	LDW	-96.4	-12.1	Small air bubble
2019-09-13	Sep-19	9	256	12:46	7TW	-112.3	-14.3	NA
2019-09-19	Sep-19	9	262	9:53	CTW	-109	-13.9	NA
2019-09-19	Sep-19	9	262	10:06	KSO2	-110.5	-14.1	NA
2019-09-19	Sep-19	9	262	10:32	SAF2	-113.2	-14.5	NA
2019-09-19	Sep-19	9	262	10:52	PAN	-105.6	-13.3	NA
2019-09-19	Sep-19	9	262	11:08	WAG	-92.5	-11.3	NA
2019-09-19	Sep-19	9	262	11:29	SAF3	-112.1	-14.4	NA
2019-09-19	Sep-19	9	262	11:55	WAG2	-107.6	-13.6	NA
2019-09-20	Sep-19	9	263	11:29	DUT	-92.6	-11.2	NA
2019-09-20	Sep-19	9	263	11:36	LEE	-76.4	-8.9	Small air bubble
2019-09-20	Sep-19	9	263	12:05	LDA	-93.6	-11.5	Small air bubble
2019-09-20	Sep-19	9	263	12:26	LDE	-88.9	-10.9	Small air bubble
2019-09-20	Sep-19	9	263	12:38	HHAR	-94.7	-11.6	NA
2019-09-26	Sep-19	9	269	10:20	7TW	-111.6	-14.2	NA
2019-09-26	Sep-19	9	269	10:32	KSO	-116.9	-15.3	NA
2019-09-26	Sep-19	9	269	11:10	WAL2	-116.2	-15.2	NA
2019-09-26	Sep-19	9	269	11:28	WAL	-111.8	-14.4	NA
2019-09-26	Sep-19	9	269	11:43	PAN2	-109.4	-13.8	NA

2019-09-27	Sep-19	9	270	9:46	TLR	-24.5	-4.2	NA
2019-09-27	Sep-19	9	270	11:55	SHEL	-110.6	-14.4	NA
2019-09-27	Sep-19	9	270	12:05	LENA	-101	-13.1	NA
2019-09-27	Sep-19	9	270	12:23	WEIR	-103.3	-13.2	NA
2019-09-27	Sep-19	9	270	12:32	DRY	-105.7	-13.6	NA
2019-09-27	Sep-19	9	270	12:43	LAKE	-112.1	-14.6	NA
2019-09-27	Sep-19	9	270	13:02	PHP	-20.1	-2.7	NA
2019-09-27	Sep-19	9	270	13:22	LDF	-104	-13.2	NA
2019-09-27	Sep-19	9	270	13:34	LDW	-102.7	-12.7	NA
2019-09-30	Sep-19	9	273	9:18	DUT	-89.6	-10.7	NA
2019-09-30	Sep-19	9	273	9:35	LEE	-84.3	-10	NA
2019-09-30	Sep-19	9	273	10:10	BIG	-95.7	-12.2	NA
2019-09-30	Sep-19	9	273	10:45	LDA	-100.8	-12.6	NA
2019-09-30	Sep-19	9	273	11:10	LDE	-95.2	-11.9	NA
2019-09-30	Sep-19	9	273	11:23	HHAR	-97.1	-11.7	NA
2019-09-30	Sep-19	9	273	12:30	GABE2	-116.7	-15.2	Gabe Bowen - Project ID: 00225
2019-09-30	Sep-19	9	273	13:21	GABE3	-116.3	-15.1	Gabe Bowen - Project ID: 00225
2019-09-30	Sep-19	9	273	14:32	GABE4	-117.1	-15.2	Gabe Bowen - Project ID: 00225
2019-09-30	Sep-19	9	273	14:42	GABE5	-116.7	-15.2	Gabe Bowen - Project ID: 00225
2019-09-30	Sep-19	9	273	14:56	GABE6	-116.7	-15.1	Gabe Bowen - Project ID: 00225
2019-09-30	Sep-19	9	273	15:08	GABE7	-116.8	-15.2	Gabe Bowen - Project ID: 00225

2019-09-30	Sep-19	9	273	15:21	GABE8	-116.7	-15.2	Gabe Bowen - Project ID: 00225
2019-09-30	Sep-19	9	273	15:32	GABE9	-114.8	-14.9	Gabe Bowen - Project ID: 00225
2019-09-30	Sep-19	9	273	15:51	GABE10	-114.9	-14.9	Gabe Bowen - Project ID: 00225
2019-09-30	Sep-19	9	273	16:09	GABE11	-116.5	-15.1	Gabe Bowen - Project ID: 00225
2019-09-30	Sep-19	9	273	16:20	GABE12	-118.0	-15.4	Gabe Bowen - Project ID: 00225
2019-09-30	Sep-19	9	273	16:29	GABE13	-117.5	-15.3	Gabe Bowen - Project ID: 00225
2019-09-30	Sep-19	9	273	17:17	GABE14	-117.7	-15.3	Gabe Bowen - Project ID: 00225
2019-09-30	Sep-19	9	273	17:22	GABE15	-117.7	-15.3	Gabe Bowen - Project ID: 00225
2019-09-30	Sep-19	9	273	17:28	GABE16	-117.7	-15.2	Gabe Bowen - Project ID: 00225
2019-09-30	Sep-19	9	273	17:39	GABE17	-118.0	-15.3	Gabe Bowen - Project ID: 00225
2019-09-30	Sep-19	9	273	17:57	GABE18	-113.1	-14.5	Gabe Bowen - Project ID: 00225
2019-09-30	Sep-19	9	273	18:06	GABE19	-128.5	-17.1	Gabe Bowen - Project ID: 00225
2019-09-30	Sep-19	9	273	18:11	GABE20	-128.5	-17.2	Gabe Bowen - Project ID: 00225
2019-09-30	Sep-19	9	273	18:19	GABE21	-129.7	-17.4	Gabe Bowen - Project ID: 00225
2019-09-30	Sep-19	9	273	18:31	GABE22	-124.6	-16.5	Gabe Bowen - Project ID: 00225
2019-09-30	Sep-19	9	273	18:44	GABE23	-121.7	-16.0	Gabe Bowen - Project ID: 00225

2019-09-30	Sep-19	9	273	18:52	GABE24	-124.1	-16.4	Gabe Bowen - Project ID: 00225
2019-09-30	Sep-19	9	273	19:11	GABE25	-117.9	-15.3	Gabe Bowen - Project ID: 00225
2019-10-01	Oct-19	10	274	10:35	SAF2	-111.3	-14.2	NA
2019-10-01	Oct-19	10	274	11:01	PAN	-110.6	-14.1	NA
2019-10-01	Oct-19	10	274	11:14	WAG	-82.8	-9.7	NA
2019-10-01	Oct-19	10	274	11:33	SAF3	-107.9	-13.8	NA
2019-10-01	Oct-19	10	274	11:53	WAG2	-113.5	-14.6	NA
2019-10-01	Oct-19	10	274	12:20	CTW	-118.2	-15.3	NA
2019-10-01	Oct-19	10	274	12:34	KSO2	-113.3	-14.6	NA

Table A2. Extended stream sampling site details (part 1).

Abbr.	Sampling Location Latitude	Sampling Location Longitude	Lat/Long Datum	Water Provider 1	Water Provider 1 Coverage (%)
BIG	39.5633216	-104.927758	NAD83	CENT	45
DRY	39.734375	-105.0395556	NAD83	CMWC	80
DUT	39.6001111	-105.0419222	NAD83	DEN	95
HCOL	39.66920278	-104.9425083	NAD83	DEN	100
HHAR	39.6717222	-104.9770278	NAD83	DEN	100
LAKE	39.73519444	-105.0313611	NAD83	CMWC	51
LEE	39.5961111	-105.0160278	NAD83	DEN	93
LENA	39.74040278	-105.1488333	NAD83	CMWC	39
LDA	39.5937361	-104.9065	NAD83	DEN	100
LDE	39.6491542	-104.9788705	NAD83	DEN	97
LDF	39.81936667	-105.0214472	NAD83	ARV	51
LDW	39.82655278	-105.0400639	NAD83	ARV	59
SWOM	39.8778035	-105.1816145	WGS84	NA	NA
WOM	39.884711	-105.18121	WGS84	NA	NA
WEIR	39.7172472	-105.0420111	NAD83	DEN	76

Table A3. Extended stream sampling site details (part 2).

Abbr.	Water Provider 2	Water Provider 2 Coverage (%)	Water Provider 3	Water Provider 3 Coverage (%)
BIG	DEN	4	NA	NA
DRY	DEN	20	NA	NA
DUT	NA	NA	NA	NA
HCOL	NA	NA	NA	NA
HHAR	NA	NA	NA	NA
LAKE	DEN	47	NA	NA
LEE	CENT	7	NA	NA
LENA	GOLD	28	DEN	2
LDA	NA	NA	NA	NA
LDE	CENT	2	NA	NA
LDF	WEST	38	DEN	7
LDW	WEST	37	NA	NA
SWOM	NA	NA	NA	NA
WOM	NA	NA	NA	NA
WEIR	CMWC	24	NA	NA

Table A4. Extended stream sampling site details (part 3).

Abbr.	Minimum Watershed Elevation (m)	Mean Watershed Elevation (m)	Maximum Watershed Elevation (m)	Watershed Elevation Range (m)
BIG	1730.7	1847.1	2006.6	275.9
DRY	1600.3	1665.4	1733.2	132.9
DUT	1633.1	1771.8	2422.6	789.5
HCOL	1641.4	1673.1	1718.7	77.3
HHAR	1620.0	1659.8	1718.7	98.7
LAKE	1591.0	1718.2	2064.0	473.0
LEE	1636.5	1696.1	1758.0	121.6
LENA	1707.7	1891.5	2317.2	609.6
LDA	1705.5	1747.6	1785.2	79.8
LDE	1623.0	1725.1	1921.2	298.2
LDF	1592.8	1660.3	1748.4	155.5
LDW	1606.8	1670.4	1748.4	141.6
SWOM	1752.3	1841.5	1905.9	153.6
WOM	1746.7	1857.2	1952.1	205.3
WEIR	1614.0	1690.0	1837.4	223.4

Table A5. Extended stream sampling site details (part 4).

Abbr.	Mean Watershed Slope	Modeled Imperviousness (%)	StreamStats Imperviousness (%)	StreamStats Dr. Area (30m DEM) (km^2)
BIG	5.5	22	22	29.0
DRY	2.0	42	46	8.9
DUT	5.9	26	25	38.1
HCOL	2.1	36	40	5.1
HHAR	2.1	32	38	10.3
LAKE	3.8	34	38	40.7
LEE	3.6	29	31	6.3
LENA	9.3	24	22	23.5
LDA	3.3	44	43	3.7
LDE	3.6	29	29	61.4
LDF	2.6	35	NA	NA
LDW	2.6	33	35	26.9
SWOM	4.3	1	NA	7.4
WOM	4.4	5	3	NA
WEIR	2.8	32	40	14.4

Table A6. Extended precipitation and tap sampling site details (part 1).

Abbr.	Site ID	Site Name	Sampling Location Latitude
PHP	PRECIP1	Anonymous Urban Farm	39.763915
TLR	PRECIP2	City of Westminster Tree Limb Recycling Center	39.880044
TW	TAP1	Chipotle	39.734049
NTW	TAP2	Noodles and Co.	39.585971
TBTW	TAP3	Taco Bell	39.842206
STW	TAP4	Santiago's	39.753752
7TW	TAP5	7-Eleven	39.82759
CTW	TAP6	Conoco	39.6729807
STTW	TAP7	Supiva Thai	39.698089
NGTW	TAP8	Natural Grocers	39.679054
MDTW	TAP9	McDonald's	39.710733
CKTW	TAP10	New China Kitchen	39.720765
BBTW	TAP11	Farm House at Breckenridge Brewery	39.593671
SAF	TAP12	Safeway	39.883551
DINO	TAP13	Sinclair	39.733253
CIRK	TAP14	Circle K	39.609188
KSO	TAP15	King Sooper's	39.843591
TAR	TAP16	Target	39.707792
WAL	TAP17	Walmart	39.722203
WAL2	TAP18	Walmart	39.742679
SHEL	TAP19	Shell	39.731653
SAF2	TAP20	Safeway	39.59636

PAN	TAP21	Panera Bread	39.556165
WAG	TAP22	Walgreen's	39.541833
SAF3	TAP23	Safeway	39.574871
TAR2	TAP24	Target	39.610876
KSO2	TAP25	King Sooper's	39.666765
MD2	TAP26	McDonald's	39.566981
WAG2	TAP27	Walgreen's	39.610151
PAN2	TAP28	Panera Bread	39.705113
GABE1	GABE1	Denver International Airport	39.85894492
GABE2	GABE2	Denver International Airport	39.85894492
GABE3	GABE3	UNO	39.77335464
GABE4	GABE4	Circle K	39.59553323
GABE5	GABE5	Walgreens	39.59546152
GABE6	GABE6	Conoco	39.61343898
GABE7	GABE7	Phillips 66	39.61033605
GABE8	GABE8	Starbucks	39.6231441
GABE9	GABE9	Burger King	39.68105678
GABE10	GABE10	McDonalds	39.68211366
GABE11	GABE11	Burger King	39.67821437
GABE12	GABE12	7-Eleven	39.67825523
GABE13	GABE13	Sinclair	39.67796163
GABE14	GABE14	7 Lenguas	39.74037058
GABE15	GABE15	7-Eleven	39.74052581
GABE16	GABE16	Circle K	39.74062679
GABE17	GABE17	Illegal Petes	39.74002751
GABE18	GABE18	7-Eleven	39.74057137
GABE19	GABE19	Arbys	39.74082324
GABE20	GABE20	Circle K	39.74527562
GABE21	GABE21	Safeway	39.77153869
GABE22	GABE22	Exxon	39.79577847
GABE23	GABE23	Starbucks	39.8167268
GABE24	GABE24	Wendys	39.85601128
GABE25	GABE25	Dairy Queen	39.91349062

Table A7. Extended precipitation and tap sampling site details (part 2).

Abbr.	Sampling Location Longitude	Lat/Long Datum	Sample Type	Water Provider
PHP	-105.022848	WGS84	PRECIP	NA
TLR	-105.155859	WGS84	PRECIP	NA
TW	-105.160032	WGS84	TAP	CMWC
NTW	-105.026245	WGS84	TAP	DEN
TBTW	-105.055309	WGS84	TAP	ARV
STW	-105.0255	WGS84	TAP	DEN
7TW	-105.034733	WGS84	TAP	WEST
CTW	-104.9732645	WGS84	TAP	DEN
STTW	-105.025478	WGS84	TAP	DEN
NGTW	-104.942448	WGS84	TAP	DEN

MDTW	-105.023494	WGS84	TAP	DEN
CKTW	-105.024835	WGS84	TAP	DEN
BBTW	-105.025025	WGS84	TAP	DEN
SAF	-105.022641	WGS84	TAP	WEST
DINO	-105.053525	WGS84	TAP	DEN
CIRK	-105.037136	WGS84	TAP	DEN
KSO	-105.056394	WGS84	TAP	ARV
TAR	-105.078873	WGS84	TAP	DEN
WAL	-105.080527	WGS84	TAP	CMWC
WAL2	-105.079513	WGS84	TAP	CMWC
SHEL	-105.168519	WGS84	TAP	CMWC
SAF2	-104.903485	WGS84	TAP	DEN
PAN	-104.881719	WGS84	TAP	DEN
WAG	-104.912218	WGS84	TAP	CENT
SAF3	-104.991872	WGS84	TAP	DEN
TAR2	-105.101902	WGS84	TAP	DEN
KSO2	-104.936876	WGS84	TAP	DEN
MD2	-104.92365	WGS84	TAP	DEN
WAG2	-105.109333	WGS84	TAP	DEN
PAN2	-105.080662	WGS85	TAP	DEN
GABE1	-104.6739259	WGS84	TAP	DEN
GABE2	-104.6739259	WGS84	TAP	DEN
GABE3	-104.7964444	WGS84	TAP	DEN
GABE4	-104.902515	WGS84	TAP	DEN
GABE5	-104.9615353	WGS84	TAP	DEN
GABE6	-104.9992608	WGS84	TAP	DEN
GABE7	-105.0826033	WGS84	TAP	DEN
GABE8	-105.1095906	WGS84	TAP	DEN
GABE9	-105.1196281	WGS84	TAP	DEN
GABE10	-105.0262013	WGS84	TAP	DEN
GABE11	-104.9867032	WGS84	TAP	DEN
GABE12	-104.9684129	WGS84	TAP	DEN
GABE13	-104.9226488	WGS84	TAP	DEN
GABE14	-104.8889982	WGS84	TAP	DEN
GABE15	-104.8990744	WGS84	TAP	DEN
GABE16	-104.9237683	WGS84	TAP	DEN
GABE17	-104.9630141	WGS84	TAP	DEN
GABE18	-105.0327046	WGS84	TAP	DEN
GABE19	-105.0666463	WGS84	TAP	CMWC
GABE20	-105.0809874	WGS84	TAP	CMWC
GABE21	-105.0806954	WGS84	TAP	CMWC
GABE22	-105.0770631	WGS84	TAP	ARV
GABE23	-105.0811829	WGS84	TAP	ARV
GABE24	-105.0809891	WGS84	TAP	ARV
GABE25	-104.996207	WGS84	TAP	WEST

Table A8. Duplicate samples.

Date	Abbreviation	δ^2H	$\delta^{18}O$	Notes
2018-09-10	DRY	-93.4	-11.9	Improper Crimping
2018-09-10	DRY	-92.7	-11.8	Improper Crimping
2018-09-10	LDW	-102.4	-12.9	Improper Crimping
2018-09-10	LDW	-102.5	-13.0	Improper Crimping
2018-09-10	LAKE	-98.8	-12.5	Improper Crimping
2018-09-10	LAKE	-99.9	-12.8	Improper Crimping
2018-09-10	LENA	-95.2	-12.3	Improper Crimping
2018-09-10	LENA	-95.7	-12.4	Improper Crimping
2018-09-10	TW	-109.9	-14.3	Improper Crimping
2018-09-10	TW	-110.3	-14.6	Improper Crimping
2018-09-10	WEIR	-104.0	-13.1	Improper Crimping
2018-09-10	WEIR	-103.1	-12.8	Improper Crimping

Table A9. Missing samples.

Date	Abbr.
2019-03-09	BIG
2019-03-09	LDW
2019-03-09	TBTW
2019-08-01	DUT
2019-08-08	HCOL

Table A10. Unknown sample.

Abbreviation	δ^2H	$\delta^{18}O$	Notes
UNKNOWN	-67.7	-8	This sample is either HCOL (2019-08-08) or DUT (2019-08-01)

Table A11. Water provider losses (part 1).

Water Provider	Distributed Water	Metered Water	Calculated Loss	Calculated Loss Units
ARV	17559	17367	192	acre-ft/yr
CENT	5089881	5052670	37211	gal, thous/yr
DEN	198165	183870	14295	acre-ft/yr
GOLD	3340	2967	373	acre-ft/yr
WEST	6133600	5305510	828090	gal, thous/yr

Table A12. Water provider losses (part 2).

Water Provider	Water Provider Service Area	Service Area Units	Area-Normalized Mean Flow (mm/d)	Percent Loss (%)	Notes
ARV	25956	acres	0.0062	1.1	NA
CENT	22	mi^2	0.0068	0.7	NA
DEN	9.31E+08	m^2	0.052	7.2	Loss estimates for most of CMWC service area were included in this report.
GOLD	22508564	m^2	0.056	11.2	NA
WEST	34	mi^2	0.0068	13.5	NA

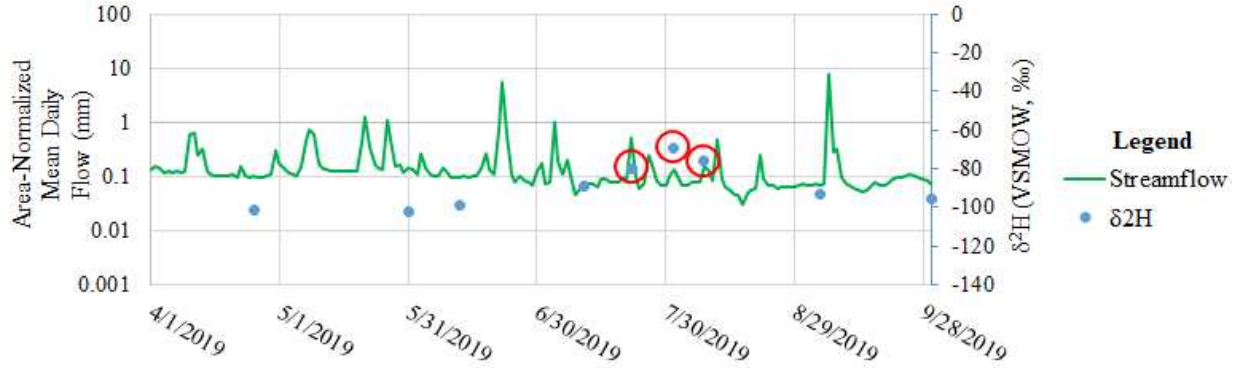

Figure A1. Hydrographs for mean daily streamflow and measured δ^2H isotope values for watershed BIG. Samples that may not be baseflow are circled in red.

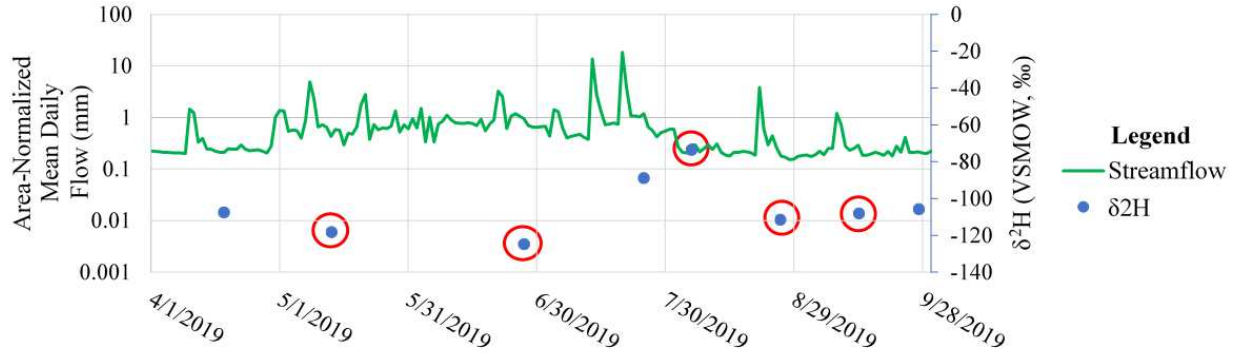

Figure A2. Hydrographs for mean daily streamflow and measured δ^2H isotope values for watershed DRY. Samples that may not be baseflow are circled in red.

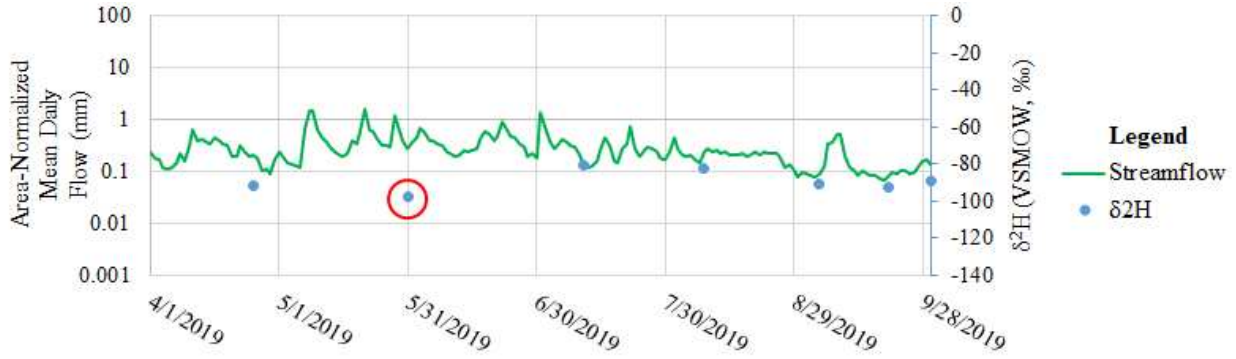

Figure A3. Hydrographs for mean daily streamflow and measured δ^2H isotope values for watershed DUT. Samples that may not be baseflow are circled in red.

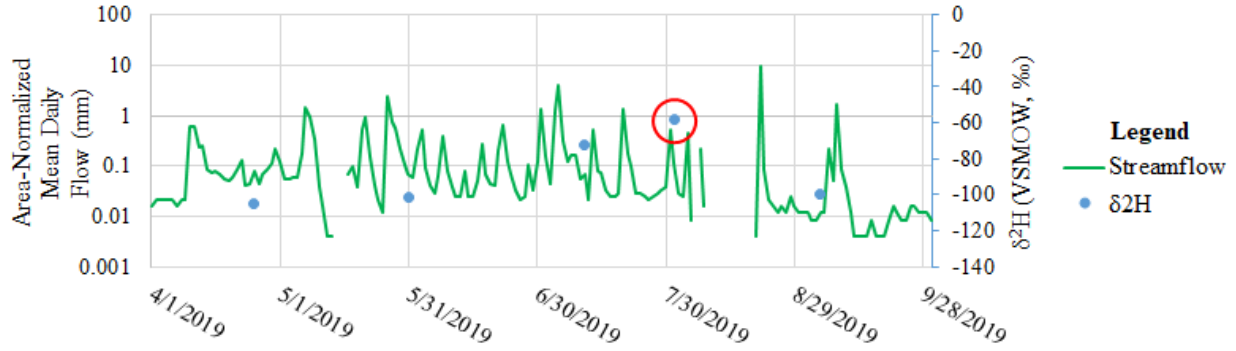

Figure A4. Hydrographs for mean daily streamflow and measured δ^2H isotope values for watershed HCOL. Samples that may not be baseflow are circled in red.

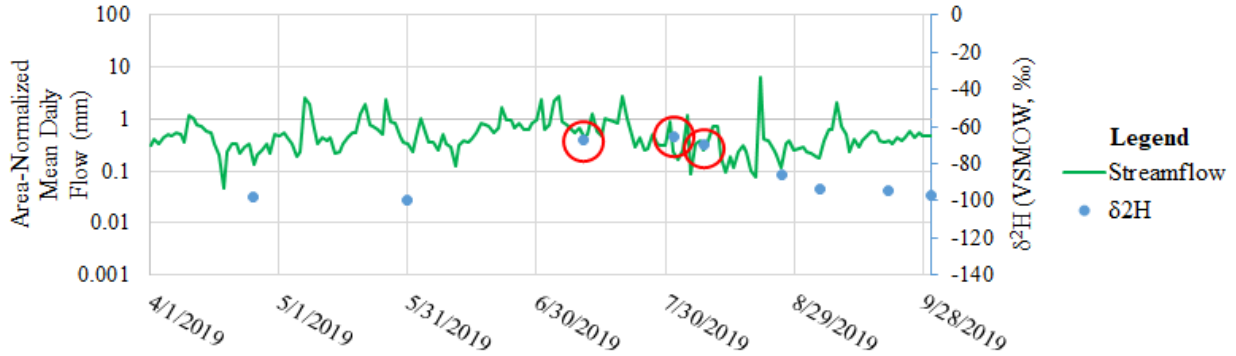

Figure A5. Hydrographs for mean daily streamflow and measured δ^2H isotope values for watershed HHAR. Samples that may not be baseflow are circled in red.

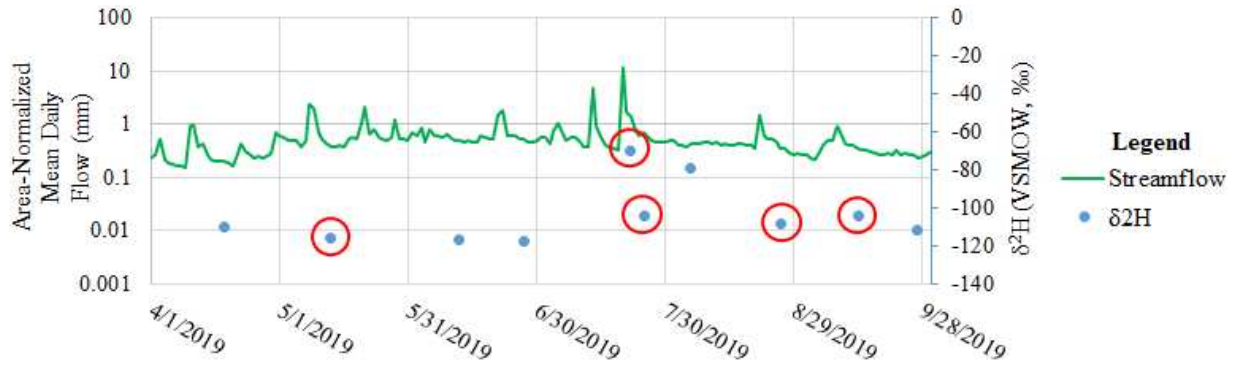

Figure A6. Hydrographs for mean daily streamflow and measured δ^2H isotope values for watershed LAKE. Samples that may not be baseflow are circled in red.

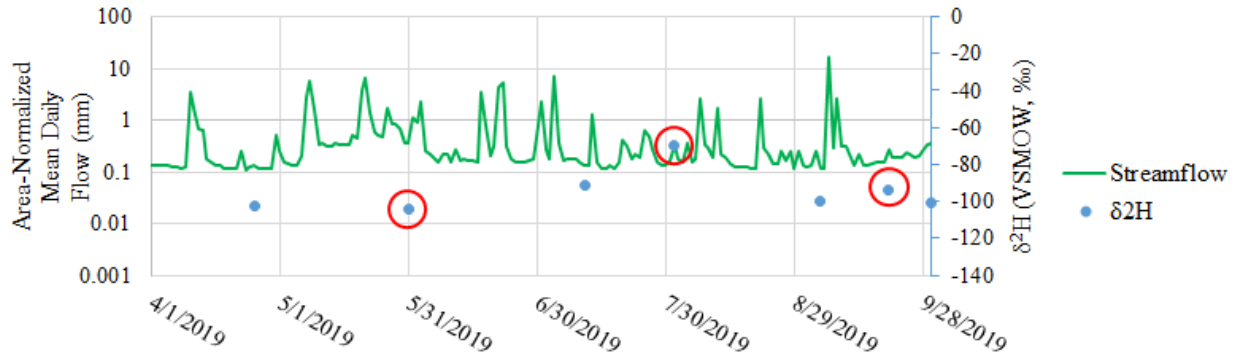

Figure A7. Hydrographs for mean daily streamflow and measured δ^2H isotope values for watershed LDA. Samples that may not be baseflow are circled in red. The final point appears to be responding to a storm event, but we verified that the stormflow occurred after the sample was taken.

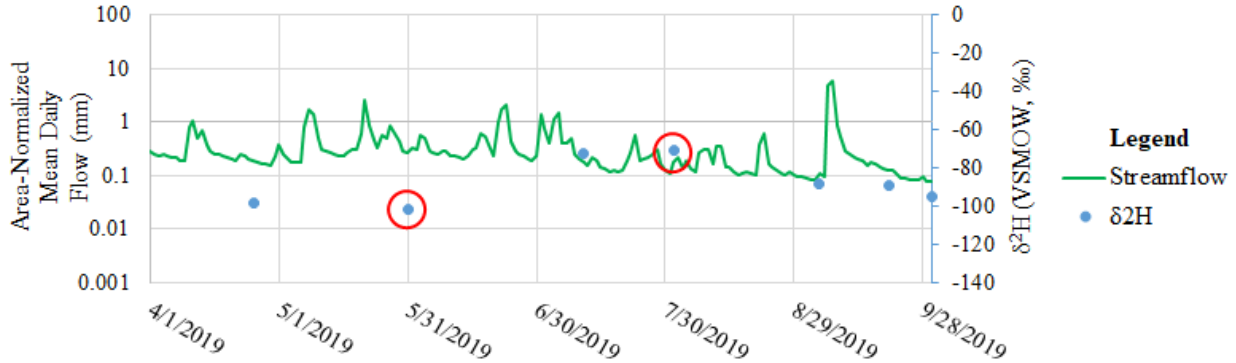

Figure A8. Hydrographs for mean daily streamflow and measured δ^2H isotope values for watershed LDE. Samples that may not be baseflow are circled in red.

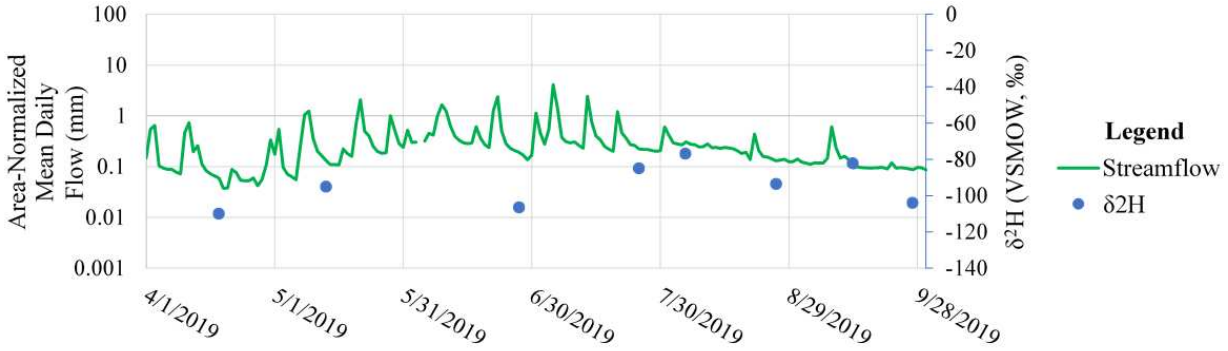

Figure A9. Hydrographs for mean daily streamflow and measured δ^2H isotope values for watershed LDF.

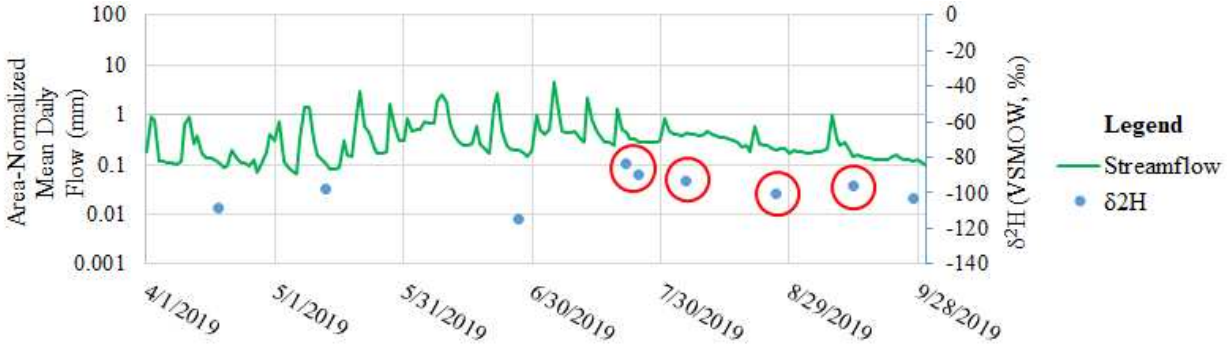

Figure A10. Hydrographs for mean daily streamflow and measured δ^2H isotope values for watershed LDW. Samples that may not be baseflow are circled in red.

Figure A11. Hydrographs for mean daily streamflow and measured δ^2H isotope values for watershed LEE. Samples that may not be baseflow are circled in red.

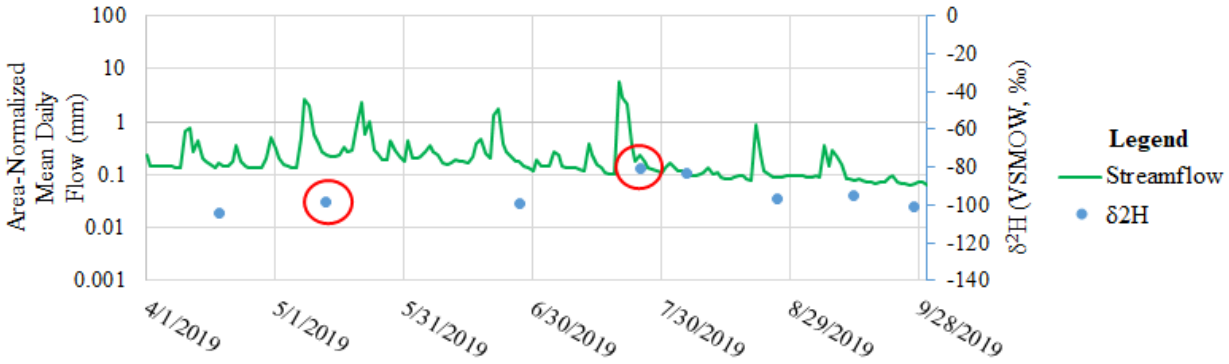

Figure A12. Hydrographs for mean daily streamflow and measured δ^2H isotope values for watershed LENA. Samples that may not be baseflow are circled in red.

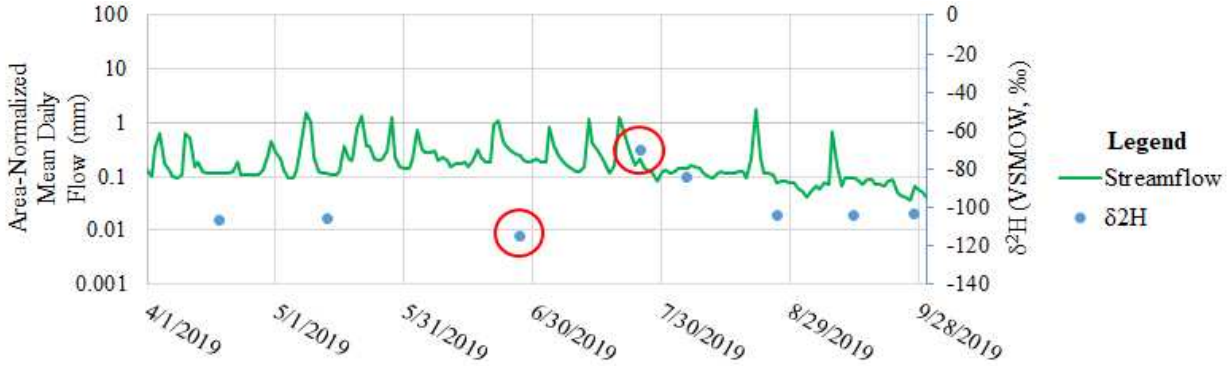

Figure A13. Hydrographs for mean daily streamflow and measured δ^2H isotope values for watershed WEIR. Samples that may not be baseflow are circled in red. The final point appears to be responding to a storm event, but we verified that the stormflow occurred after the sample was taken.

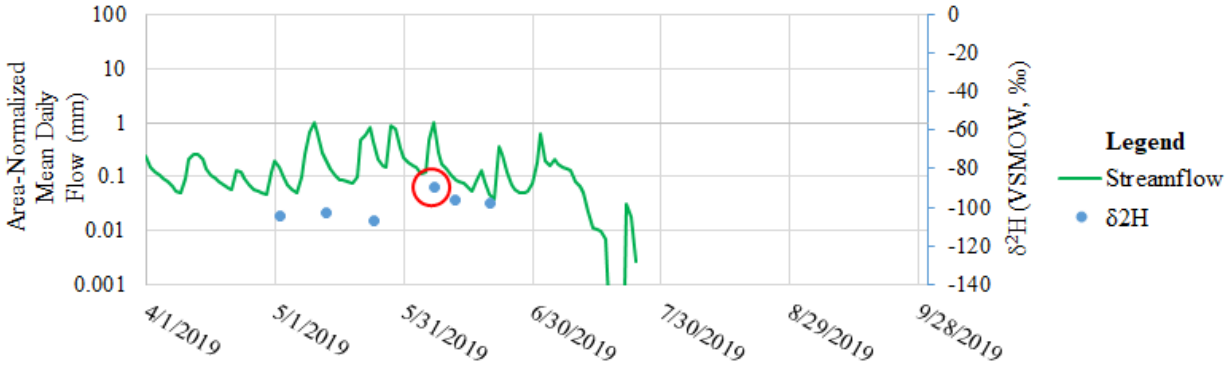

Figure A14. Hydrographs for mean daily streamflow and measured δ^2H isotope values for watershed WOM. Samples that may not be baseflow are circled in red.

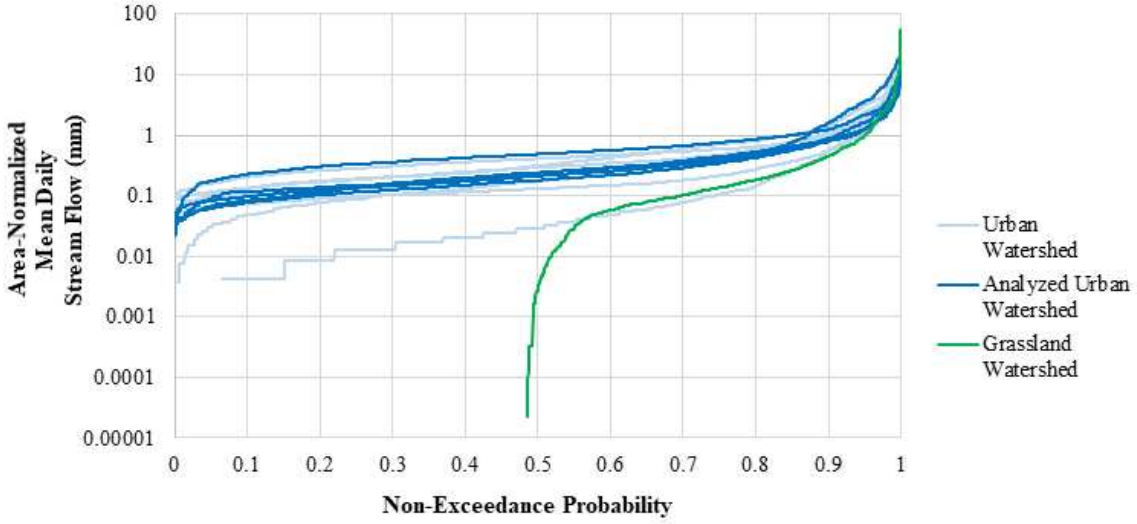

Figure A15. Non-exceedance probabilities for the 2013 - 2019 area-normalized mean daily streamflow in the Denver metropolitan area. Zero flow and unreported flow days are not shown on the logarithmic y-axis. Time frame is June 7, 2013 – September 30, 2013 and April 1 – September 30 for years 2014, 2015, 2016, 2017, 2018, 2019.

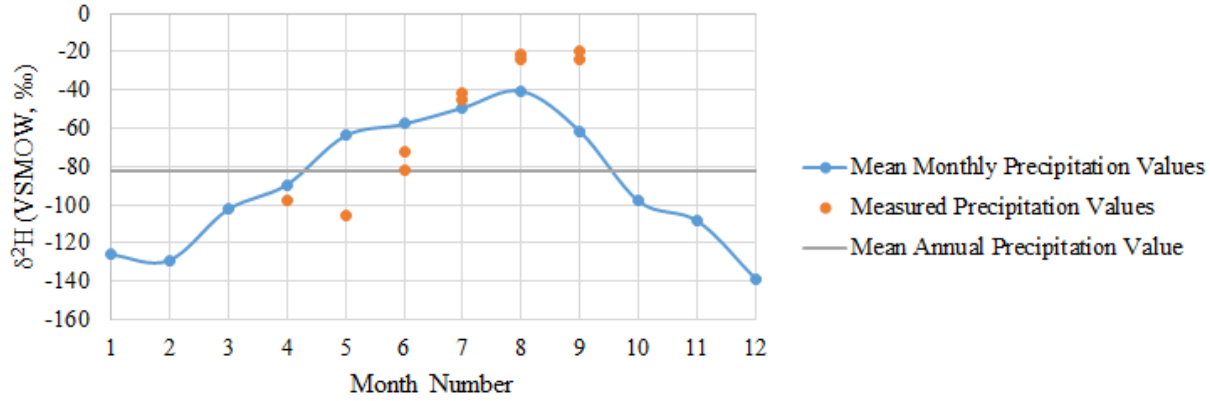

Figure A16. Comparing our measured precipitation δ^2H values to the mean monthly and mean annual precipitation δ^2H values.

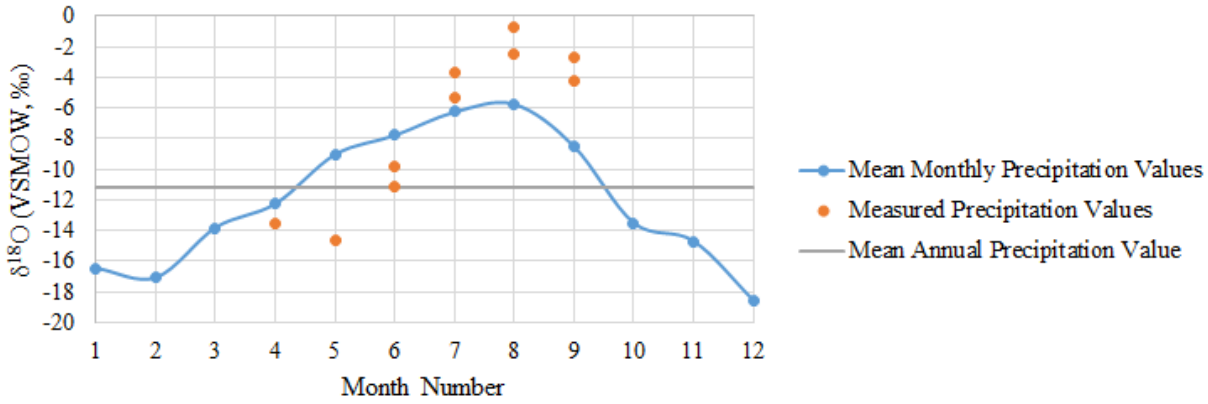

Figure A17. Comparing our measured precipitation $\delta^{18}O$ values to the mean monthly and mean annual precipitation $\delta^{18}O$ values.